

UNCLASSIFIED

AD 433791

DEFENSE DOCUMENTATION CENTER

FOR

SCIENTIFIC AND TECHNICAL INFORMATION

CAMERON STATION, ALEXANDRIA, VIRGINIA



UNCLASSIFIED

NOTICE: When government or other drawings, specifications or other data are used for any purpose other than in connection with a definitely related government procurement operation, the U. S. Government thereby incurs no responsibility, nor any obligation whatsoever; and the fact that the Government may have formulated, furnished, or in any way supplied the said drawings, specifications, or other data is not to be regarded by implication or otherwise as in any manner licensing the holder or any other person or corporation, or conveying any rights or permission to manufacture, use or sell any patented invention that may in any way be related thereto.

64-11

433791

RADC-TDR-63-510

HIGH POWER R-F WINDOW STUDY PROGRAM

FINAL TECHNICAL REPORT

NOVEMBER, 1963

VARIAN ASSOCIATES
PALO ALTO, CALIFORNIA

CONTRACT NO. AF 30(602)-2844

Prepared For

ROME AIR DEVELOPMENT CENTER
AIR FORCE SYSTEMS COMMAND
RESEARCH AND TECHNOLOGY DIVISION
UNITED STATES AIR FORCE
GRIFFISS AIR FORCE BASE
NEW YORK

DDC
RECEIVED
APR 2 1964

VARIAN REPORT NO. 304-1F

NOVEMBER, 1963

433791

CATALOGED BY DDC

AS AD NO. _____

This report has been released to the Office of Technical Services, U. S. Department of Commerce, Washington 25, D.C. , for sale to the general public.

DDC AVAILABILITY NOTICE

Qualified Requestors May Obtain Copies Of This Report From DDC

PATENT NOTICE: When Government drawings, specifications, or other data are used for any purpose other than in connection with a definitely related Government procurement operation, the United States Government thereby incurs no responsibility or any obligation whatsoever and the fact that the Government may have formulated, furnished, or in any way supplied the said drawings, specifications or other data is not to be regarded by implication or otherwise as in any manner licensing the holder or any other person or corporation, or conveying any rights or permission to manufacture, use or sell any patented invention that may in any way be related thereto.



VARIAN associates

611 HANSEN WAY • PALO ALTO, CALIF.

RADC-TDR-63-510

HIGH POWER R-F WINDOW STUDY PROGRAM

FINAL TECHNICAL REPORT

November, 1963

VARIAN ASSOCIATES

Palo Alto, California

Contract No. AF 30(602)-2844

Project No. 5573

Task No. 557303

Prepared by: Floyd Johnson

Approved by: L. T. Zitelli

D. G. Dow

Prepared For

ROME AIR DEVELOPMENT CENTER
AIR FORCE SYSTEMS COMMAND
RESEARCH AND TECHNOLOGY DIVISION
UNITED STATES AIR FORCE
GRIFFISS AIR FORCE BASE
NEW YORK

VARIAN REPORT NO. 304-1F

Copy No. 176

This report has been released to the Office of Technical Services, U. S. Department of Commerce, Washington 25, D.C., for sale to the general public.

DDC AVAILABILITY NOTICE

Qualified Requestors May Obtain Copies Of This Report From DDC

PATENT NOTICE: When Government drawings, specifications, or other data are used for any purpose other than in connection with a definitely related Government procurement operation, the United States Government thereby incurs no responsibility or any obligation whatsoever and the fact that the Government may have formulated, furnished, or in any way supplied the said drawings, specifications or other data is not to be regarded by implication or otherwise as in any manner licensing the holder or any other person or corporation, or conveying any rights or permission to manufacture, use or sell any patented invention that may in any way be related thereto.

FOREWORD

a. The current trend toward development of higher average power capabilities in microwave tubes has repeatedly shown the design of ceramic output windows to be one of the more serious problem areas. The objective of this effort was to develop a high average power microwave window capable of passing power levels considerably beyond the current state of the art. A goal of 250 kilowatts of CW power at twenty-five percent bandwidth was established.

b. The major portion of the program consisted of experimental evaluation of numerous window designs in a high power resonant ring. Window configurations included thin and thick discs, resonant blocks, and double thin discs surface cooled with dielectric liquid. Window materials included the alumina and beryllia ceramics, quartz, boron nitride and synthetic sapphire. As a result of the experiments, two specific window designs were found to be superior for use with large amounts of average power. These are the thin disc window made of synthetic sapphire and the resonant block window made of beryllium oxide. Each of these windows repeatedly withstood the maximum available test power of 260 kilowatts. These two windows exhibited 20 and 25 percent bandwidth respectively.

c. Another portion of this effort consisted of developing a technique for design of disc and block windows by computer. This effort was quite successful in that windows designed by this technique have very nearly the anticipated characteristics. Fortran II Statements for these computer techniques are included in the 4th Quarterly Report under this contract (RADC-TDR-63-349).

d. Information gained as a result of this contract will be useful in the design of any microwave tube required to generate large amounts of average power. The data will be of specific immediate use in the development of a one-megawatt CW X-band klystron now under contract by the Air Force.

/s/Dirk T. Bussey
Project Engineer
RADC Griffiss AFB NY

ABSTRACT

The purpose of the work undertaken by this study program was to pursue theoretical and experimental investigations leading to the development, fabrication and testing of windows with bandwidths up to 25 per cent and capable of transmitting 250 kilowatts cw, X-band power. Considerations of bandwidth and power requirements limited fabrication of test models to windows using single and double discs and self resonant block windows.

Double disc windows allowed cooling by fluid dielectrics and permitted broadband, ghost mode free operation. The maximum power actually transmitted through any of the models of this window was 180 kilowatts. Restricted fluid flow paths limited the amount of cooling available and thus limited further increases in power. Further design work on this window might be indicated considering the generally good results obtained with it.

The program requirements were more than satisfied by the high power testing to 275 kilowatts of a single crystal sapphire disc window. In all, three different sapphire windows were tested without window failure to powers of 250 kilowatts or more.

Three beryllium oxide self resonant (half wavelength) block windows also survived powers in excess of 250 kilowatts. Test conditions for beryllia and sapphire windows included those of full pressurization or evacuated on one side and pressurized on the other. No windows using either beryllia or sapphire were fractured due to excessive power during this program.

Aluminum oxide ceramic windows of either the thin disc or block configurations were shown to fracture at 100 kilowatts or less in any configuration tested. The power level attained in high purity alumina block windows was very little higher than that attained in less pure varieties of the same ceramic.

In the light of test results from beryllia and alumina block windows, it becomes apparent that thermal conductivity is more important than ceramic purity. The higher purity ceramics are stronger and less lossy, but the gain is not sufficient to outweigh low thermal conductivity.

Compression sealed thin disc quartz windows were melted by r-f heating at power levels as low as 50 kilowatts. The best optical grade fused quartz became extremely hot at 190 kilowatts but did not deform. Despite the substantially improved performance of the better quality quartz, this material seems to offer little as a high average-power window.

The possibility of designing thin disc and block type window assemblies analytically was thoroughly investigated. As a result, computer programs have been written which can be used to optimize window designs with a minimum of time and expense.

The effects of stray magnetic fields and variations of vacuum pressure on initiating the phenomena of multipactor were also investigated. The conclusion drawn from these experiments is that multipactor is not a problem at power levels up to 250 kilowatts cw.

PUBLICATION REVIEW

This report has been reviewed and is approved. For further technical information on this project, contact

Approved:

Dirk T. Bussey
DIRK T. BUSSEY
Project Engineer

Approved:

Arthur J. Frohlich
ARTHUR J. FROHLICH
Ch, Techniques Branch
Surveillance & Control

FOR THE COMMANDER:

Irving J. Gabelman
IRVING J. GABELMAN
Chief, Advanced Studies Group

TABLE OF CONTENTS

<u>Section</u>	<u>Page No.</u>
I INTRODUCTION	1
1-1. CONTRACTUAL INFORMATION	1
1-2. RESEARCH AND ENGINEERING OBJECTIVES AND ACCOMPLISHMENTS	1
II DISCUSSION	4
2-1. PERFORMANCE OF HIGH POWER CW WINDOWS AS A FUNCTION OF MATERIALS AND CONFIGURATIONS.	4
A. General Considerations	4
B. Half-Wavelength Block Windows	5
1. Beryllium Oxide Block Windows	5
2. Aluminum Oxide Block Windows	8
C. Single Thin Disc Windows	13
1. Sapphire Single Discs	13
2. Aluminum Oxide Single Discs	20
3. Boron Nitride Single Discs	20
4. Fused Quartz Single Discs	26
D. Double Thin Disc Windows	33
1. Temperature Limitations and Cooling Methods	33
2. Fluid Cooled Double Discs	33
3. Gas Cooled Double Discs	40
2-2. WINDOW DESIGN	46
A. Broad Banding of Half-Wavelength Blocks - Impedance Match and Mode Freedom	46
B. Window Synthesis	46
1. Half-Wavelength Block Window Components	50
2. Dielectric Cooled Disc Window Components	52
3. Computation of Window Characteristics	56
2-3. OBSERVATIONS ON MULTIPACTOR AND EVACUATED WINDOWTRON OPERATION	64
A. Conductive Coatings	64
B. Vacuum Testing	65
C. Effects of Stray Magnetic Fields	69

TABLE OF CONTENTS, Cont.

<u>Section</u>		<u>Page No.</u>
	2-4. TEMPERATURE GRADIENTS IN WINDOWS	69
	2-5. RING RESONATOR CONSIDERATIONS	71
III	CONCLUSIONS	74
IV	RECOMMENDATIONS	77
	REFERENCES	78

LIST OF ILLUSTRATIONS

<u>Figure</u>		<u>Page No.</u>
1A	HIGH POWER WINDOW TEST ASSEMBLY	6
1B	VSWR CHARACTERISTICS OF A TYPICAL BERYLLIA BLOCK WINDOW WHERE $F_o = 7.75$ Gc	7
2	POWER DISSIPATION IN VARIOUS BERYLLIUM OXIDE WINDOWS	10
3	POWER DISSIPATED IN BERYLLIA-SAPPHIRE WINDOWTRON . .	11
4	MEASURED BROADBANDED BeO BLOCK WINDOW CHARACTERISTICS	12
5	THERMAL FAILURES OF TWO AL955 HALF-WAVELENGTH BLOCK WINDOWS	14
6	THERMAL FAILURES OF HALF-WAVELENGTH BLOCK AL300 and AL399 WINDOWS	15
7	POWER DISSIPATED IN VARIOUS ALUMINA WINDOWS	16
8	ILLUSTRATION OF CERAMIC FAILURE DUE TO TRANSMISSION OF TM_{11} MODE	18
9	SHOWING THE EFFECT OF INCREASING A THIN DISC WINDOW ASSEMBLY LENGTH	19
10	VSWR CHARACTERISTICS OF 1.250-INCH DIAMETER SAPPHIRE WINDOW TESTED TO 263 KILOWATTS IN WINDOWTRON	21
11	POWER DISSIPATION IN SINGLE CRYSTAL SAPPHIRE WINDOWS (MEASURED CALORIMETRICALLY)	22
12	SINGLE DISC SAPPHIRE WINDOW ASSEMBLY USED AS ONE HALF OF WINDOWTRON	23
13	AVERAGE DISSIPATION IN SINGLE THIN DISC AL300 WINDOWS .	24
14	ILLUSTRATING RADIAL CRACKS OF FAILURE ON OPPOSITE SIDES OF A THIN DISC ALUMINA WINDOW	25
15	SINGLE DISC BORON NITRIDE WINDOW CHARACTERISTICS VSWR VS FREQUENCY	28
16	AVERAGE DISSIPATION IN THIN DISC FUSED QUARTZ WINDOWS	29
17	FAILURE OF FUSED QUARTZ WINDOW NO. 1	30

LIST OF ILLUSTRATIONS, Cont.

<u>Figure</u>		<u>Page No.</u>
18	FAILURE OF FUSED QUARTZ WINDOW NO. 2	31
19	CROSS SECTIONS OF R-F MELTED FUSED QUARTZ BUBBLE	32
20	POWER DISSIPATION IN VARIOUS DOUBLE DISC FC-75 COOLED WINDOW ASSEMBLIES	37
21	DISASSEMBLED FC-75 COOLED WINDOW SHOWING HIGH TEMPERATURE FAILURE (PRESSURIZED SIDE FAILED). . .	38
22	CROSS-SECTIONS OF DOUBLE DISC WINDOWS	39
23	HIGH POWER FC-75 COOLED DOUBLE DISC WINDOW	41
24	VSWR CHARACTERISTICS OF A DOUBLE DISC AL300 WINDOW WITH CONICAL TRANSITIONS	42
25	DOUBLE DISC AL300 WINDOW ASSEMBLY (a) FINAL ASSEMBLY (b) FULL SCALE CROSS-SECTIONAL SKETCH . .	43
26	DISASSEMBLED DOUBLE DISC WINDOW NO. 1 CERAMICS SHOWING HIGH TEMPERATURE FAILURE	44
27	POWER DISSIPATION IN DOUBLE DISC AL300 WINDOW WITH AND WITHOUT DRY NITROGEN COOLING	45
28	MODE FREQUENCY PLOT FOR AL300 BLOCK WINDOWS . . .	47
29	MODE FREQUENCY PLOT FOR BERYLLIA BLOCK WINDOW . .	48
30	WINDOW CONFIGURATION MODELS SHOWING CONTRIBUTIONS OF MATRIX COMPONENTS [a] THROUGH [k]	49
31	SCATTERING MATRIX COEFFICIENT VALUES FOR 1.4-INCH DIAMETER TO WR112 WAVEGUIDE TRANSITION	55
32	FOUR TERMINAL NETWORK REPRESENTATION OF A WAVEGUIDE WINDOW	56
33	BERYLLIUM OXIDE WINDOW ACTUAL AND COMPUTER MODELS	58
34	MEASURED AND COMPUTED RESULTS FROM BROADBAND BERYLLIUM OXIDE WINDOW	60
35	COMPUTED AND MEASURED VSWR CHARACTERISTICS OF A THIN DISC λ_g LONG, CYLINDRICAL WINDOW	61

LIST OF ILLUSTRATIONS, Cont.

<u>Figure</u>		<u>Page No.</u>
36	COMPUTED AND MEASURED VSWR CHARACTERISTICS OF A SYMONS-TYPE SINGLE DISC AL300 WINDOW	63
37	SKETCH SHOWING METHOD OF VISUALLY MONITORING ALL TEST REGIONS	66
38	COMPONENTS OF WINDOWTRON ASSEMBLY	67
39	RELATIVE TEMPERATURE GRADIENTS OF VARIOUS CERAMIC HALF-WAVELENGTH WINDOWS AT 100 Kw	70
40	TEMPELSTK MELTING CONTOURS OF BERYLLIUM OXIDE BLOCK WINDOW	72

SECTION I

INTRODUCTION

1-1. CONTRACTUAL INFORMATION

This publication is a report of all work performed under United States Air Force Contract Number AF30(602)-2844. The initiating and supervising agency was Rome Air Development Center, Griffiss Air Force Base, New York, which awarded the contract on July 6, 1962, in accordance with RADC Exhibit "A," dated 29 December 1961.

1-2. RESEARCH AND ENGINEERING OBJECTIVES AND ACCOMPLISHMENTS

The purpose of this program was to conduct theoretical and experimental investigations of methods leading to a substantial improvement in high average power waveguide windows. In particular, a need had been established for devices capable of passing high power density electromagnetic waves from an evacuated region through to a highly pressurized region with a minimum of power reflected back to the source or absorbed by the pressure barrier. The obvious application of such a device, commonly called a window, is in fabrication of reliable, extremely high power microwave amplifiers such as klystrons. Window failures on these very complex and costly amplifiers are responsible for much of the difficulty that government agencies are experiencing in maintaining and procuring certain high power systems.

In very recent years, great forward strides have been made in the advancement of the state of the art of generating very high average powers, particularly at X-band. In this band, 100 kilowatt c-w klystrons are now in production, a 1 megawatt c-w klystron is in development, and it is certain that the future will bring even higher power achievements. Window technology has barely kept pace with this rapid increase of source power.

The objectives of the present program were, in general, to improve this situation, with a specific goal of designing and testing an X-band window to a minimum of 250 kilowatts continuous wave (c-w) power. A second goal was to strive to attain this power through a window with up to 25 per cent bandwidth. Bandwidth is arbitrarily defined for windows as that frequency range over which the voltage standing wave ratio (VSWR) is less than 1.2.

The general outline for this program included an investigation of various solid dielectrics and their adaptability and desirability for use with window configurations best suited for high power transmission. Other phenomena believed to be responsible for window failure under adverse operating conditions experienced in the field were

also to be investigated. These included the effects of multipactor, stray magnetic fields, variations of gas pressure, and the relative merits of various gaseous or liquid dielectrics used for cooling window assemblies.

It was generally agreed at the beginning of the program that window failure by dielectric fracture, or failure of dielectric-to-metal seals, could be attributed to the following causes.

Thermal stresses are generated by the excessive conversion of r-f into heat energy. Two distinct mechanisms for this exist. One is multipactor, which converts r-f energy indirectly into heat through electron motion or bombardment. The other is due to conductive losses observed in any dielectric which is less than a perfect insulator.

Electromechanical stresses are generated by arcs which either begin away from the dielectric and travel to its face, or begin right at the face and cause its failure.

During this program, two completely distinctive window configurations were consistently shown to be able to pass over 250 kilowatts c-w power without damage to the window. Neither of these configurations is new, and both have been proved to have certain desirable features as opposed to many other configurations which have one or more disadvantages when considered in the light of the program requirements, --namely, bandwidth and high average power.

The intuitively rugged half-wavelength block window configuration fabricated using beryllium oxide as the dielectric was shown to be able to pass every bit of available power; the maximum available was 263 kilowatts. This power was attained with a vacuum on the power input side and with two atmospheres of pressurized nitrogen on the other. In all, three different beryllium oxide windows were tested successfully to 250 kilowatts or more.

A second configuration, equally as successful as the one above, was the single thin disc Symons-type, fabricated with single crystal sapphire as the dielectric. Three different assemblies of this window were also tested to powers in excess of 250 kilowatts. The maximum power transmitted through any one of them was 275 kilowatts with both faces of the disc pressurized with nitrogen. However, in the 263 kilowatt test described above, a sapphire disc window was in series with the beryllium oxide block, and was subjected to entirely the same punishment with the exception that the transmitted power passed from the pressurized side to the evacuated side. This same window was also used as one half of the windowtron for all of the other high power tests to be discussed later.

In all, during this program 36 window assemblies were fabricated, 27 of which were tested to failure or to the limit of the ring resonator drive system. Only the single crystal sapphire and the beryllium oxide windows survived past the 180 to 200 kilowatt power level.

Next in descending order of worth, the double disc, inert fluorocarbon cooled configuration showed the most promise. Of a total of five tested, two failed at 170-180 kilowatts, one at 90 kw (due to insufficient cooling), and the remaining two were tested to 150-160 kilowatts without failure when adequately cooled.

Several types of windows failed in the region of 100 kilowatts cw. Into this classification would fall the double thin disc, conical transition assemblies made with AL300 dielectric, and the aluminum oxide half wavelength block windows. The latter windows were made with AL300, AL995 and AL399. The particular type of alumina ceramic material did not seem to matter.

A number of test windows failed below 100 kilowatts, and these were the single disc fused quartz, single disc aluminum oxide assemblies, and the uncooled double thin disc models.

During these extensive high power testing procedures, several observations were made concerning the phenomena occurring in the evacuated portion of the ring between windows as well as in the pressurized region. The ring resonator was fitted with two viewing ports which allowed visual monitoring of the power transmission regions. Several different types of glow discharges and hot spots were seen; however, none of these could definitely be ascribed as being physical manifestations of multipactor. As a result of these studies, it is felt and concluded that multipactor is not, and has never been, a serious problem in high average power c-w windows. Two main causes of dielectric failure were determined: one was low thermal conductivity, the other low flexural strength.

Some of the early high power tests were limited by breakdown in the resonant ring drive components. This was especially true for the hybrid phase shifter used to tune out mismatches within the ring. After much constant overhaul, the solution turned out to be rather simple. Every component within the ring circuit itself must be matched perfectly ($VSWR < 1.03$) at the test frequency. After this was done, very few difficulties were experienced in turning the ring power up to the limit of the ring driver tube or power supply.

As a result of work done on this contract, windows can now be designed quite exactly by the use of a computer. Programs have been written for both thin disc and block windows and they should greatly speed the determination of exact window dimension parameters. The general terms of the program allow solutions for any size of waveguide or frequency band. It is expected that this work will save future window designers much time and expense.

SECTION II

DISCUSSION

2-1. PERFORMANCE OF HIGH POWER CW WINDOWS AS A FUNCTION OF MATERIALS AND CONFIGURATION

A. General Considerations

The criterion for engineering waveguide windows can be stated as simply the ability to construct vacuum-tight waveguide structures completely pervious to electromagnetic waves. Of course, this over-simplified statement implies an understanding of the problems of thermodynamics, fluid mechanics, chemistry and the physics of microwave propagation.

The thermodynamic problem is one of selecting the best possible dielectric material from the standpoint of r-f loss. No perfect lossless material exists and therefore the heat generated must be removed from the window. Thermal conductivity looms very important in window applications, as does the thermal expansion of the materials used. The window is made up of several completely different materials which must be united by vacuum-tight joints able to remain tight over a considerable temperature range.

The union of different materials introduces chemistry into the subject. Different applications of chemical compounds are required for the metalizing of every variety of dielectric. Some dielectrics have never been successfully sealed to metal. Others have been, but only by very difficult and often expensive unreliable procedures. Mechanical strength of the bond as well as of the dielectric material itself must be given serious consideration because of the very high pressure differentials experienced across the two faces of a window.

Chemistry is involved in waveguide windows in yet another way. Cooling of these devices can be accomplished by both gaseous and liquid dielectrics. However, these compounds must be inert or compatible with the metals involved. Their thermal conductivities and specific heats must be sufficiently high to accomplish cooling. The requirements on the electrical properties of such coolants are just as stringent as those of the solid dielectric variety. The handling of dielectric coolants in restricted regions under high pressure becomes a fluid mechanics problem.

Considering all of these aspects, as well as other somewhat less important problems, the available types of solid dielectric materials had been narrowed down to the alumina ceramics, beryllia ceramics, single crystal zero degree cut sapphire and fused quartz.⁵ The latter material would ordinarily have been disqualified because

of a very low thermal coefficient of expansion and conductivity but was retained for its other desirable properties. One additional material, single crystal synthetic beryllium oxide, will definitely have application to windows when it becomes available in large enough sizes.

The properties of the fluorocarbon liquids appeared to have promise as a vehicle for removing heat from some types of windows. Configurations adaptable are the double disc variety and the half wavelength window with fluid passages machined through the block of ceramic. Because of a loss factor, which is high by ceramic standards, a minimum exposure of these fluids to rf would be required.

These considerations, as listed in the foregoing paragraphs, are responsible for limiting the investigations of this program to half-wavelength block, thin single disc and double thin disc window configurations using the dielectric materials which were also listed.

B. Half-Wavelength Block Windows

1. Beryllium Oxide Block Windows

Just before the beginning of this program, several samples of a new isostatically pressed beryllia (B-7 body) had been obtained from the Brush Beryllia Company. This was a high density, 99.5 per cent pure material, and had a dielectric constant of 6.5. Tests on later acquisitions of an improved version of this same material (B-10 body) showed that ϵ_r equaled 6.8. According to recent communications with the Brush Co., this latter beryllia body is the standard 99.5 per cent purity material now sold by them.

The first three blocks were metalized and brazed by the standard method into watercooled waveguide assemblies as shown in Figure 1a. The ceramics used in these initial high power test pieces were not broadbanded and had a typical VSWR versus frequency curve shown in Figure 1b. The traveling wave resonant ring and driver used for high power tests were operable in the 7.7 to 7.8 GC range, so no difficulty was experienced when the half-wavelength block was cut to be resonant at 7.75 GC.

Beryllia block window No. 1 was the first window tested in this program because of these early preparations. The maximum power transmitted by it was 253 kilowatts at 7.762 GC, with 30 psi dry nitrogen pressurizing at both window faces. Arcing and breakdown within the resonant ring tuners prevented further increase of power in the ring. Subsequent microscopic inspection showed that no damage whatsoever had been done to the beryllia ceramic and there was no evidence of arcing anywhere in the ring itself.

Since several of the first beryllia windows had small seal leaks due to braze jiggling inadequacies, they were used in high power testing only to the extent that

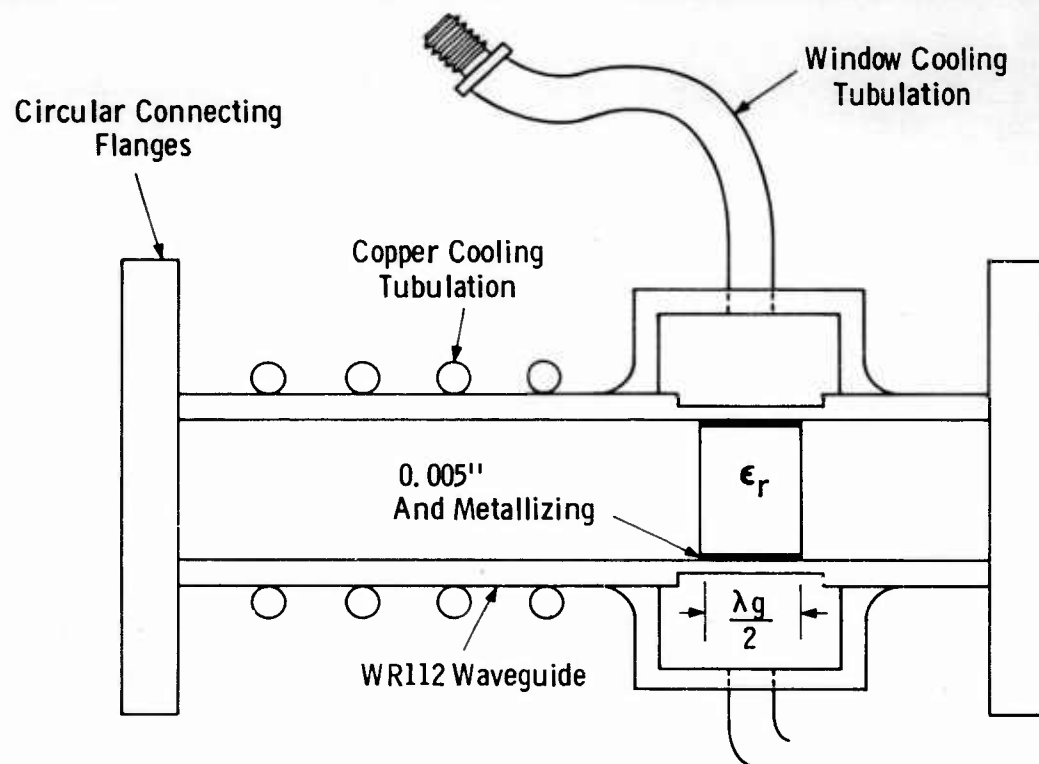


FIGURE 1A
HIGH POWER WINDOW TEST ASSEMBLY

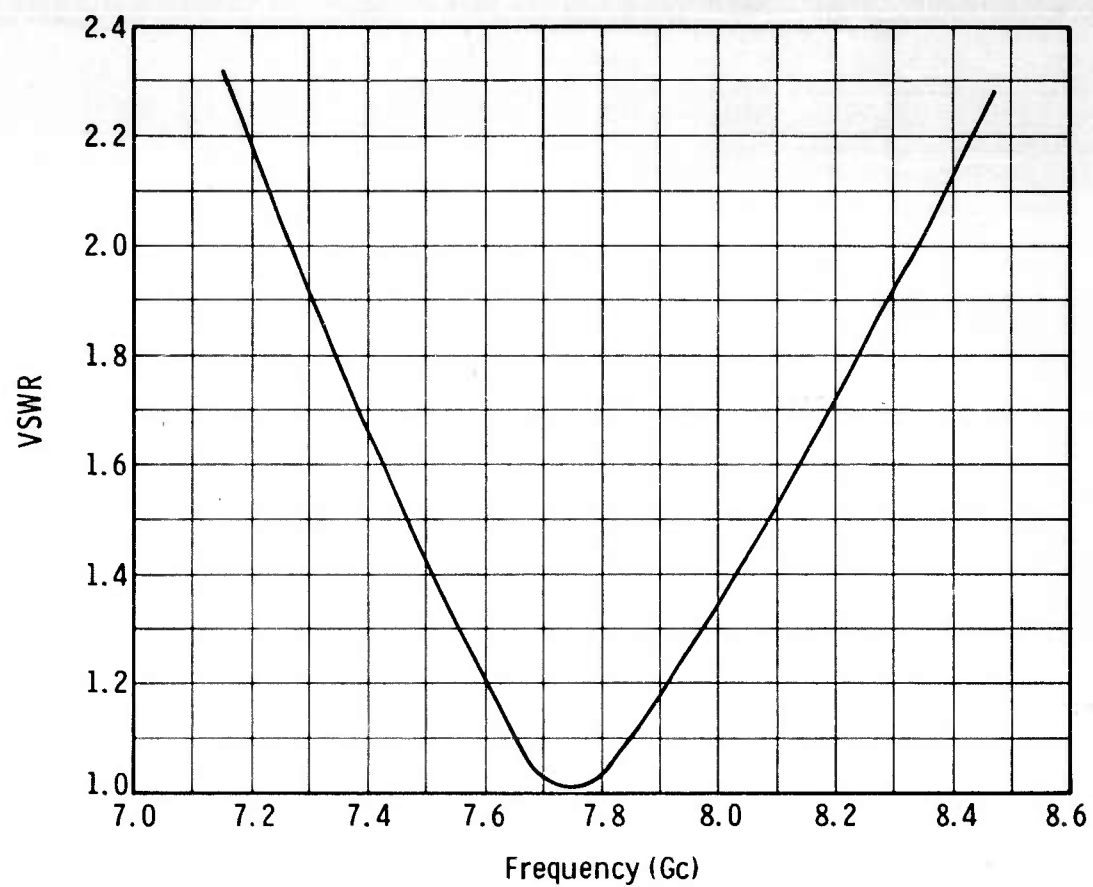


FIGURE 1B
VSWR CHARACTERISTICS OF A TYPICAL BERYLLIA BLOCK
WINDOW WHERE $F_0 = 7.75$ GC

dissipation comparisons were made. In tests described later in Section 2-4, three of these windows were used to determine temperature gradients on the face of the block. The maximum power transmitted through any of them in these tests was 210 kilowatts.

Window No. 7, as listed in Table I, was a sample of a 99.5 per cent pure beryllia supplied by National Beryllia Company. It is a hot pressed variety which is similar in its properties to the Brush Beryllia ceramics. Power tests were limited once again by ring tuning element arcing, but the window itself suffered no damage. A comparison of power dissipated in five of the beryllia windows tested is shown in Figure 2. The one sample of National Beryllia had lowest overall dissipation. The highest dissipations measured were in the Brush B-10 bodies, but it should be pointed out that seal and waveguide losses are also included in these measurements, which prevents drawing any conclusion concerning relative losses between any two beryllia bodies. The dissipation curve for window No. 8 included the losses of 4.5 inches of waveguide on either side of the window which more than doubled the measured loss. It becomes rather obvious that X-band waveguide carrying 250 kilowatts average power needs to be extremely well cooled. This latter test was made with the beryllia window in series with a sapphire disc window. The region between the windows was evacuated and continuously pumped by a VacIon® Pump. The measurements were carried out over a period of four days with power through the windows maintained at 200 to 263 kilowatts for a period of approximately 12 hours. Subsequent removal, inspection and vacuum testing of both windows showed no damage whatsoever had been done to the sapphire or beryllia. Figure 3 shows that five times more power was dissipated in the beryllia assembly than in the sapphire. However, because of the extra waveguide losses this ratio should probably be 2.5 to 3.0.

The VSWR characteristics of beryllia window No. 8 are shown in Figure 4. This window was broadbanded using dual symmetric irises on either side of the window and the block had been cut to be self-resonant at 7970 Mc. The high power test frequency was 7727 Mc. Results of this experiment would indicate that the filter network used for broadbanding is not detrimental to power handling capacity at the quarter-megawatt level despite the fact that relatively high standing waves are present between matching sections.

Beryllium oxide has proved to be an outstanding material for use as very high average power windows. None of the test windows suffered damage in any of the tests. The upper limit of this material has yet to be determined.

2. Aluminum Oxide Block Windows

The self-resonant block window has been established as one of the most reliable window configurations available. This window has been used, largely fabricated from high purity aluminas, for a wide variety of pulsed and medium to high average power tubes in most of the EIA waveguide sizes. As a result of tests made for this program, the upper power transmission limit of high purity aluminas in WR112 waveguide is indicated to be in the neighborhood of 100 kilowatts cw.

TABLE I

CONDENSED ITEMIZATION OF HIGH POWER TESTS ON
BERYLLIA HALF-WAVELENGTH BLOCK WINDOWS

<u>Window Number</u>	<u>Material</u>	<u>Maximum Test Power (kw - CW)</u>	<u>Test Conditions or Disposition</u>
1	Brush (F-7)	253	Pressurized 30 PSI Nitrogen both sides
2	Brush (F-7)	130	Temperature distribution measurements
3	Brush (F-7)	130	Temperature distribution measurements
4	Brush (B-10)	252	1st-Pressurized 30 PSI nitrogen both sides; 2nd-Vacuum one side - pressure one side
5	Brush (B-10)	210	Temperature distribution measurements
6	Brush (B-10)	0	Broad banding and cold test only
7	National BEO	222	Pressurized both sides
8	Brush (B-10)	263	Vacuum on power input side Pressure on power output side Broadband version
9	Brush (B-10)	0	Used in broadbanding experiments
10	Brush (B-10)	0	Leaky seal - Cold test only
11	Brush (B-10)	0	Leaky seal - Cold test only

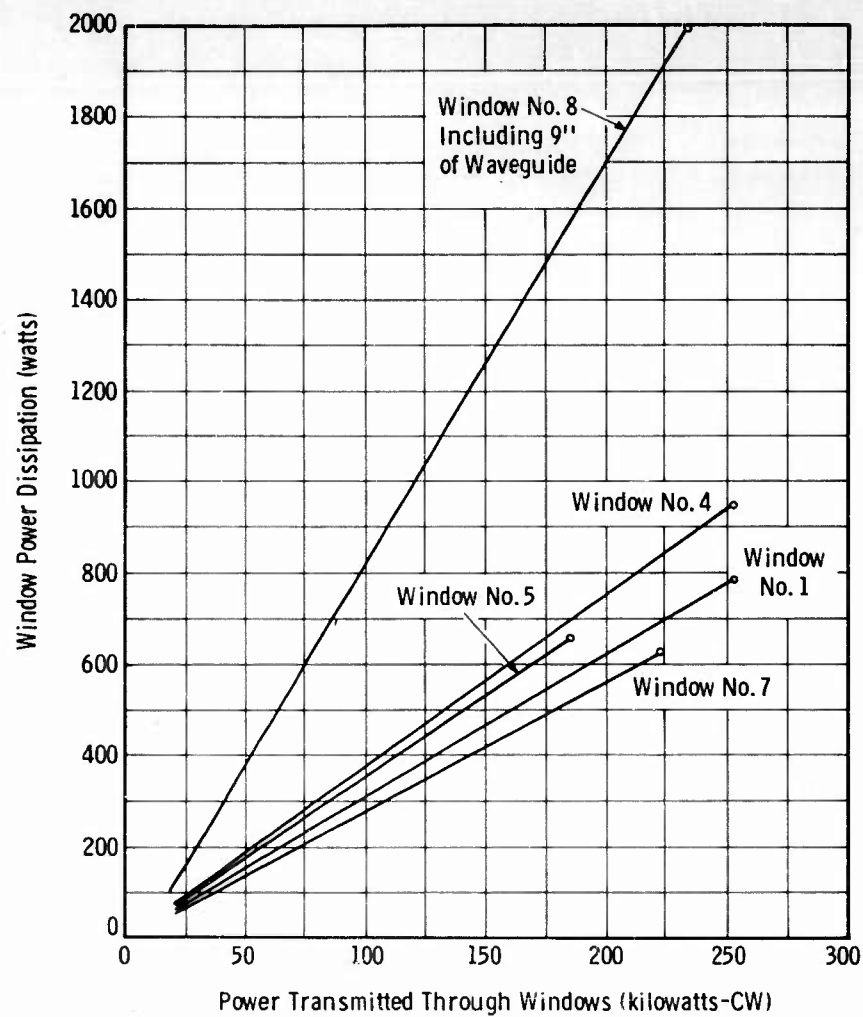


FIGURE 2
POWER DISSIPATION IN VARIOUS BERYLLIUM
OXIDE WINDOWS

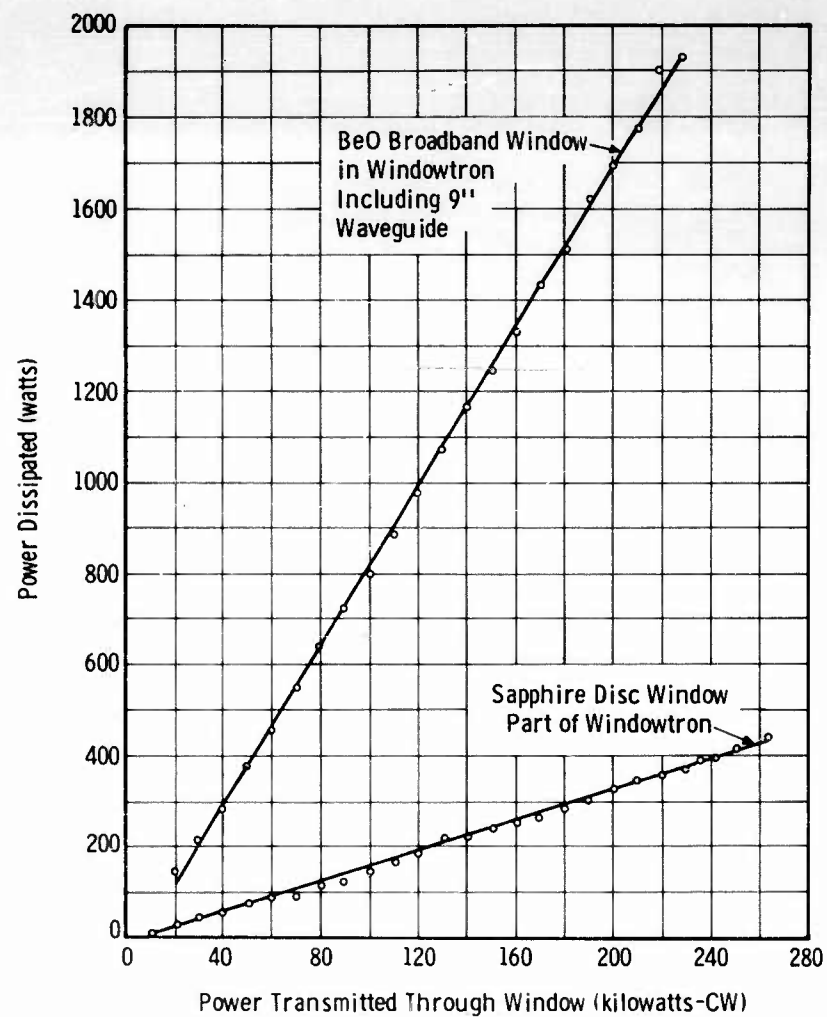


FIGURE 3
POWER DISSIPATED IN BERYLLIA-SAPPHIRE WINDOWTRON

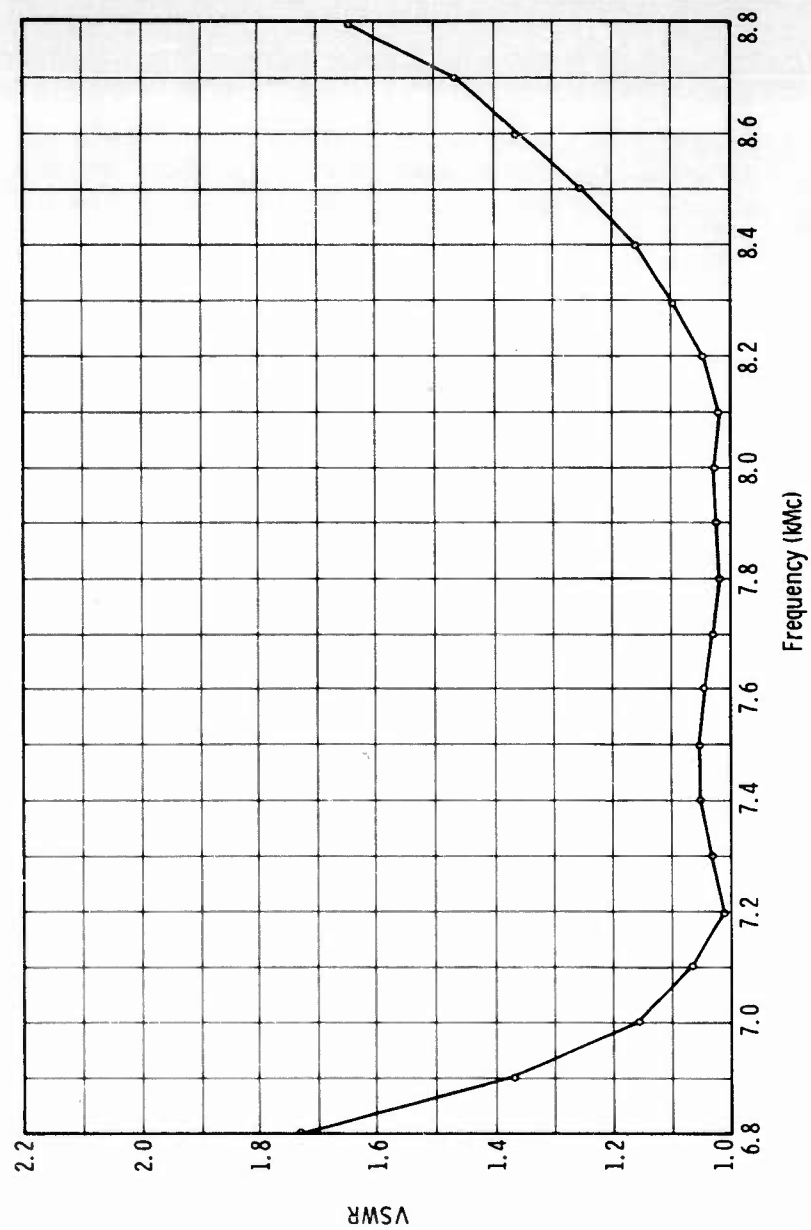


FIGURE 4
MEASURED BROADBAND BeO BLOCK
WINDOW CHARACTERISTICS

All of the block window assemblies using several varieties of alumina ceramic failed at or near 100 kilowatts. The mechanism of failure can very definitely be attributed to excessive thermally generated stresses. The nature of the failures can be seen in Figures 5 and 6 to be vertical cracks in the highest power density region of the waveguide.

Published loss tangent data would indicate that high purity aluminas are only half as lossy as an equivalent beryllia. If the same comparison is made on the thermal conductivities, the beryllias are significantly 10 times better. None of the beryllia windows failed in test at any power levels attained, whereas all of the aluminas failed. Thermal conductivity is believed to be the major and perhaps the only property of beryllia making the difference possible.

The high power alumina tests were all conducted with both faces of the window pressurized. Under these conditions, it was difficult, in the complete absence of arcing, to determine the exact power level at failure. No visible manifestations of failure could be seen. On two occasions the failure could definitely be heard as a loud cracking noise. Experimental procedure provided for removal of the window from the ring for visual inspection at about 20 kilowatts increments so that the failure level could be determined within a given range. Later testing of other assemblies with one side of the windows evacuated provided an excellent means for determining the exact power level at failure.

Approximately 3 watts of dissipated power per 1 kilowatt transmitted power were observed in the alumina windows (Figure 7) as compared to the beryllia average of 3.5 watts per kilowatt. Again, it is probably seal losses which mask the results. Differences in these two materials should theoretically be greater.

The maximum upper limit of failure was observed to be 120 kilowatts cw in any of the alumina self-resonant windows. It is recommended that this ceramic not be used for applications which approach this power level.

C. Single Thin Disc Windows

1. Sapphire Single Discs

The merits of single crystal synthetic sapphire for use as waveguide windows have been explored in previous window studies and the results of this study further confirm that this material is indeed an excellent choice for windows. In fact, the upper limit of power transmission through sapphire was not established even though one sapphire window assembly was subjected to 275 kilowatts of average power without failure.

The Symons-type configuration which uses simple abrupt transitions from rectangular to cylindrical waveguide on either side of the disc was employed as

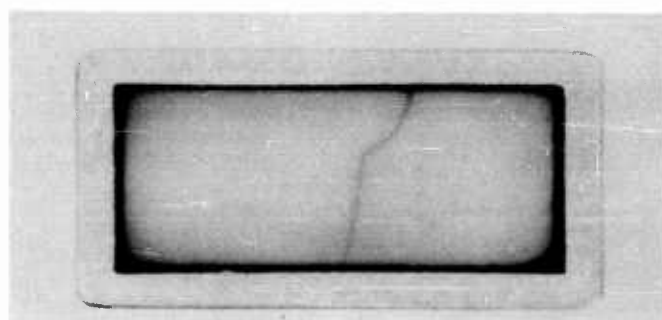
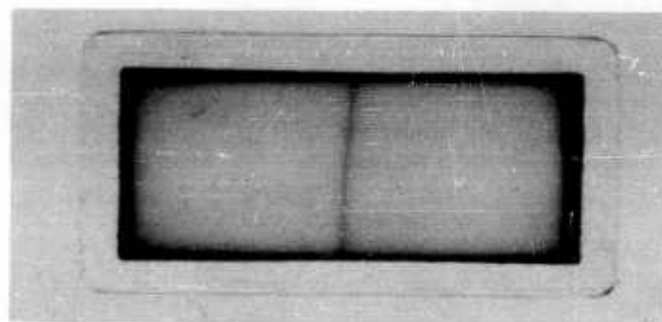
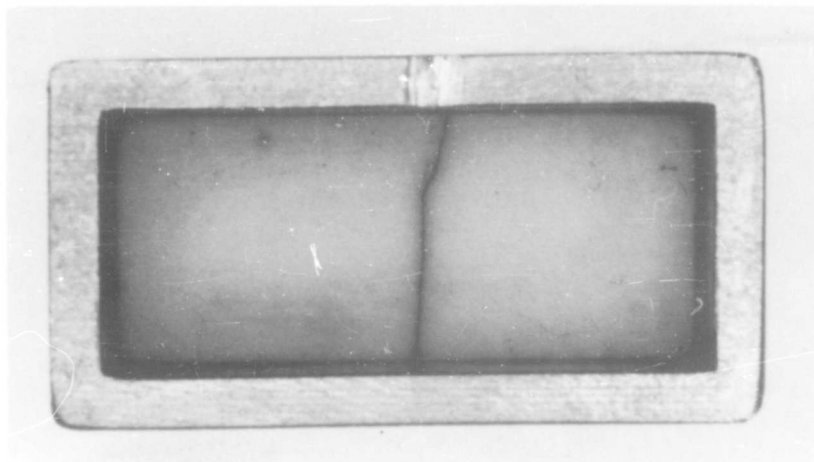
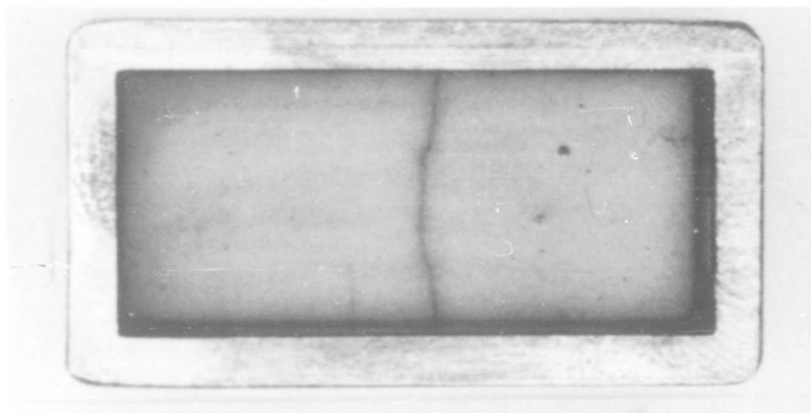


FIGURE 5
THERMAL FAILURES OF TWO AL955 HALF-WAVELENGTH
BLOCK WINDOWS



(a) AL300



(b) AL399

FIGURE 6
THERMAL FAILURES OF HALF-WAVELENGTH
BLOCK AL300 AND AL399 WINDOWS

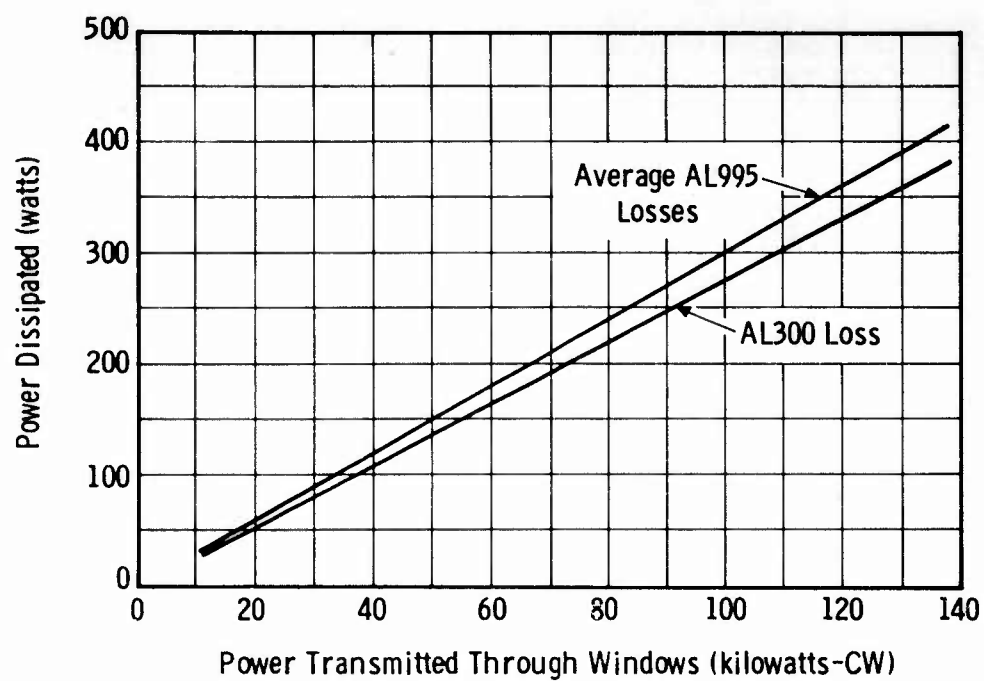


FIGURE 7
POWER DISSIPATED IN VARIOUS ALUMINA WINDOWS

a test vehicle for the sapphire thin discs. This configuration is also often identified as the "poker chip" or "pill box" window. Its advantages are that it is very broad band and it is one of the simplest to seal to metal. Generation of evanescent modes, particularly the TM_{11}^0 , by the abrupt transitions is the most serious disadvantage of this configuration. Excitation of the TM_{11}^0 mode is accompanied by normally directed electric fields at the face of the dielectric window, thus increasing the possibility of multipactor or unnecessarily concentrating power in certain regions.

Figure 8 illustrates a ceramic failure often observed in "poker chip" windows which is attributed to just this cause. As the TM_{11}^0 mode has a higher cut-off frequency than the TE_{11}^0 transmission mode, it is recommended that the diameter of the window cylinder be kept to a minimum consistent with guide size and a good broadband match. The transitions could also be moved away from the window at a sacrifice in bandwidth. This window is approximately one half-wavelength long in its usual form. Doubling the length of the structure moves the transitions far enough away so that any evanescent mode would decay before propagating to the window. Comparison is made between the bandwidths of a half-wavelength and a full wavelength "poker chip" window assembly in Figure 9.

Three single crystal, zero degree cut, synthetic sapphire windows were fabricated and successfully tested to power levels limited only by ring driver power. Table II indicates the essential data.

TABLE II

SAPPHIRE WINDOW TEST DATA

Diameter (inches)	Thickness (inches)	Total Cylindrical Length (inches)	Test Power (KW)	Test Conditions
1.400	0.050	0.532	275	Pressurized both sides 35 psi nitrogen freq. = 7750 Mc
			180	Vacuum one side in series with double disc window - double disc failed
1.330	0.050	0.464	235	Pressurized both sides - 30 psi dry nitrogen freq. = 7762 Mc
1.250	0.045	0.450	250	Retested at 7730 Mc
			263	Vacuum on one side Freq. = 7730 Mc

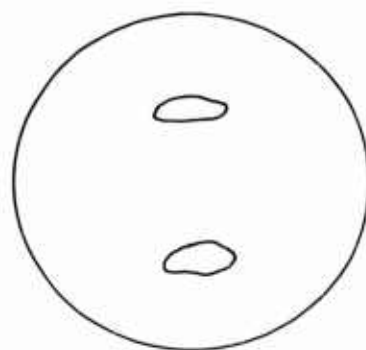


FIGURE 8
ILLUSTRATION OF CERAMIC FAILURE DUE TO
TRANSMISSION OF TM_{11} MODE

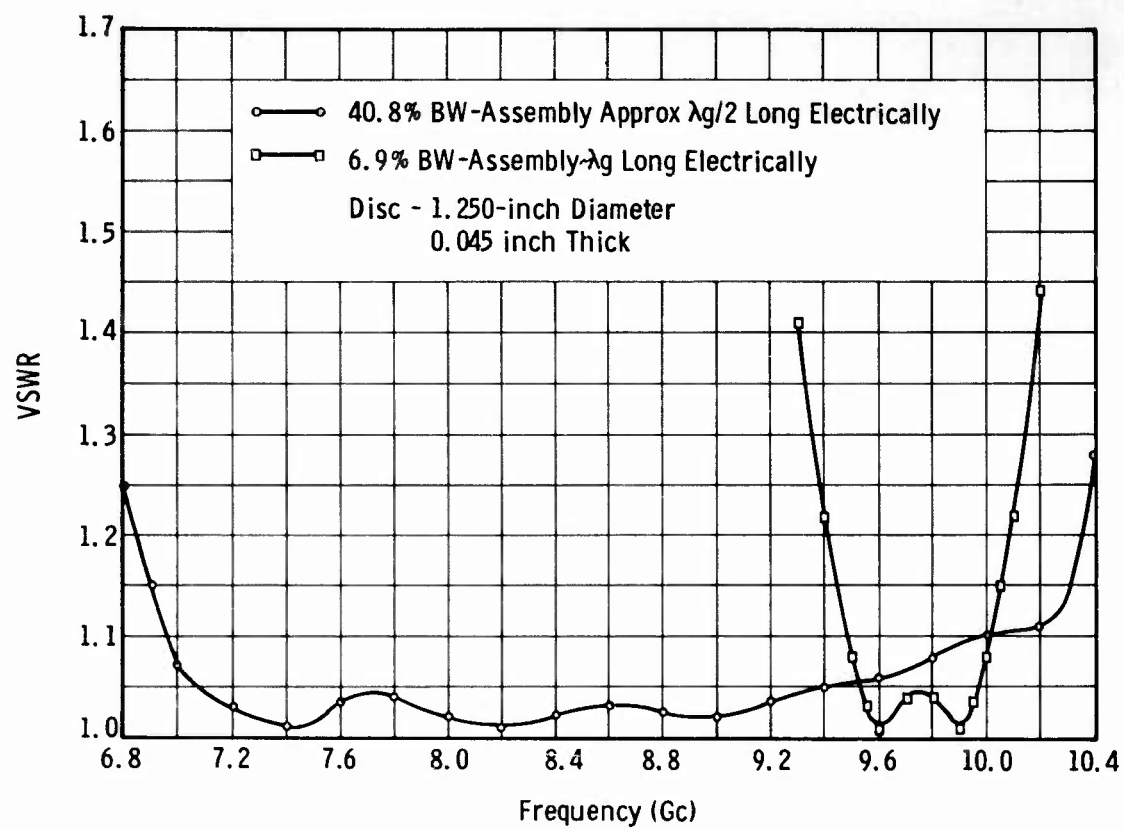


FIGURE 9
SHOWING THE EFFECT OF INCREASING A THIN DISC
WINDOW ASSEMBLY LENGTH

These windows were tested under the most difficult conditions possible, that is, with the abrupt transition within 0.250 inch or less from the sapphire disc face. They were all very broadband windows. Figure 10 illustrates the VSWR characteristics of the last sapphire window built which was tested to 263 kw in the windowtron. This window was also used in the majority of evacuated windowtron tests to be described in later sections of this report. Average dissipation in the sapphire disc window assemblies is 1.7 watts per kilowatt transmitted (Figure 11).

2. Aluminum Oxide Single Disc

Only a very small portion of the program effort was directed to building and testing the conventional Symons-type single thin disc window using ordinary sintered aluminum oxide. However, relatively cheap AL300 was used to check brazing jig dimensions in preparation for assembly of sapphire windows. As a result, two AL300 disc windows were brazed, tested and found to be vacuum-tight. The final window assemblies, identical in every respect to the sapphire versions discussed above (Figure 12), were successful also. External cooling of the window housing was done with recirculating water, just as it was for all of the high power tests with the exception of the double disc, FC-75 cooled windows.

During the last quarter, both of the AL300 single disc windows were tested to failure in the windowtron where the vacuum was maintained within a maximum of 10^{-5} Torr. Window No. 1 failed at 40 kilowatts, and No. 2 at 30 kilowatts cw. The test frequency was 7730 Mc in both cases.

An average dissipation curve is shown in Figure 13, while Figure 14 illustrates the type of radial cracks characteristic of thin disc failures. An interesting observation is that the dissipation in the disc window is identical to that of the alumina block windows, or 3 watts per kilowatts transmitted.

It appears from these tests that a very strong case can be made for the use of single crystal sapphire. In the same configuration, with every dimensional detail exactly alike, the ratio of power transmitted through sapphire and through AL300 is at least 9. However, the sapphire did not fail at the 275 kilowatt level, nor is it known just how much punishment this material will take in any given window configuration. Perhaps this ratio will eventually be proved to be much higher.

3. Boron Nitride Single Discs

Early in the program, Boron nitride was considered to have two particularly desirable properties, suggesting the possibility of its use as a thin disc window. Low loss tangent is one. Heat generated can be removed easily by circumferential cooling because of the very high thermal conductivity in the "a" or radial direction.

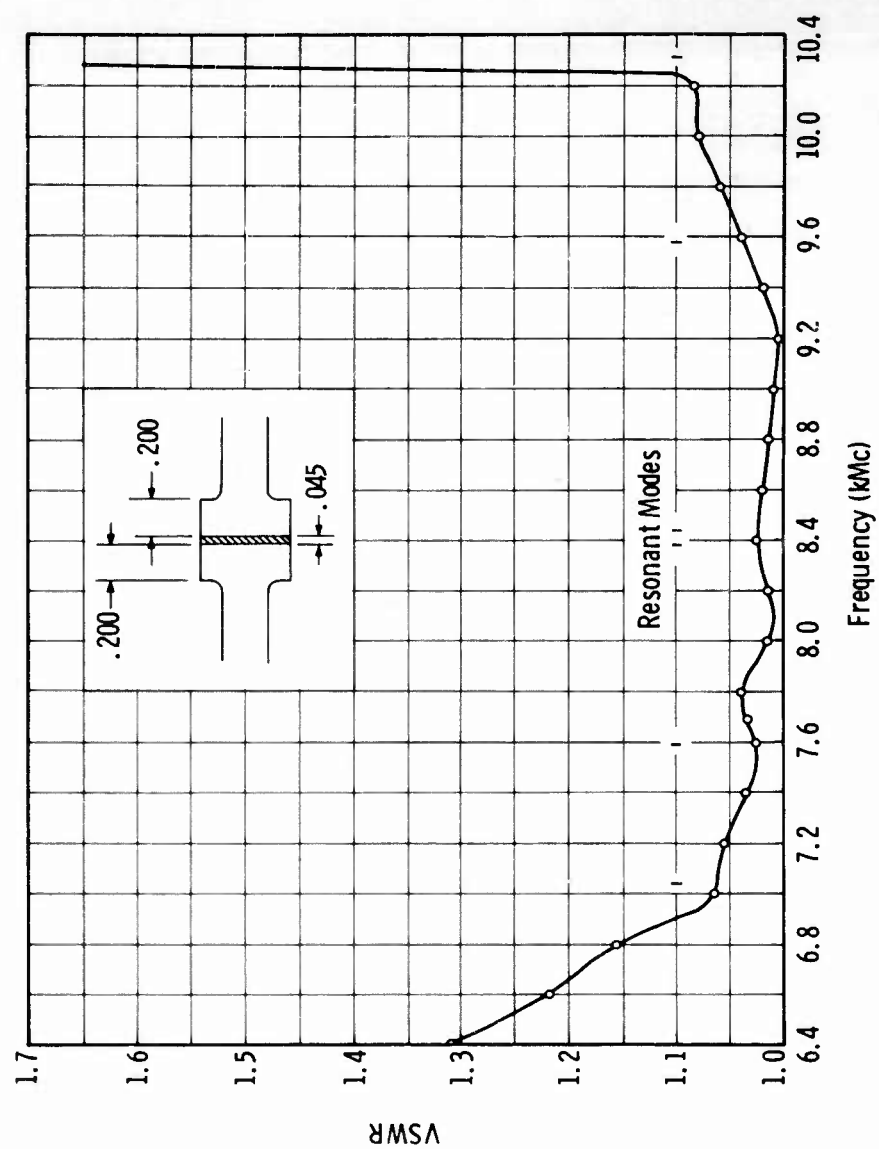


FIGURE 10
VSWR CHARACTERISTICS OF 1.250-INCH DIAMETER
SAPPHIRE WINDOW TESTED TO 263 KW IN WINDOWTRON

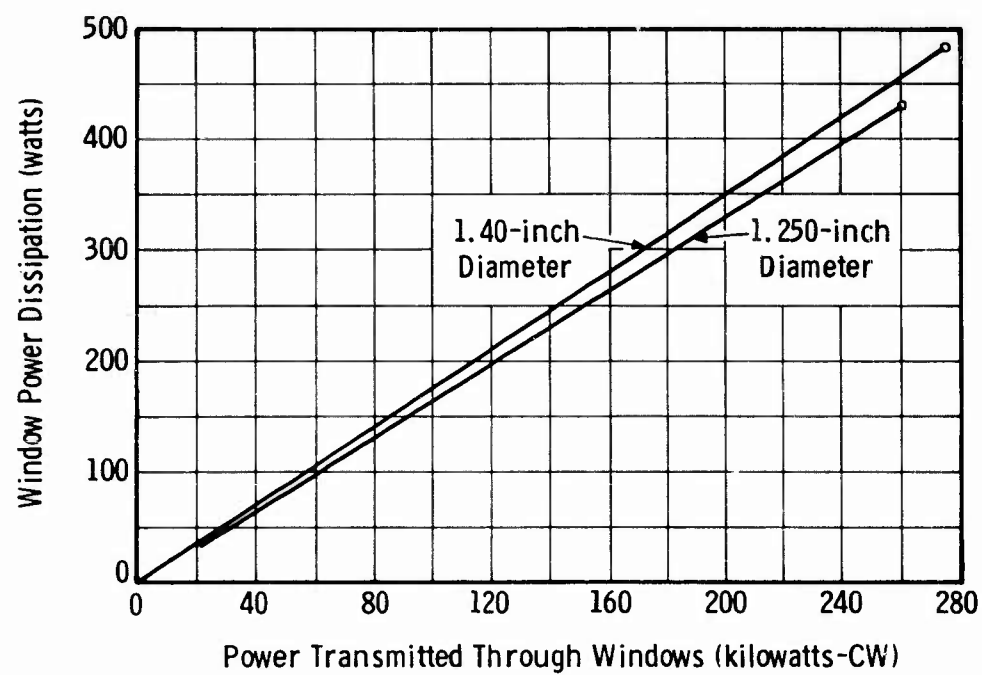


FIGURE 11
POWER DISSIPATION IN SINGLE CRYSTAL SAPPHIRE
WINDOWS (MEASURED CALORIMETRICALLY)

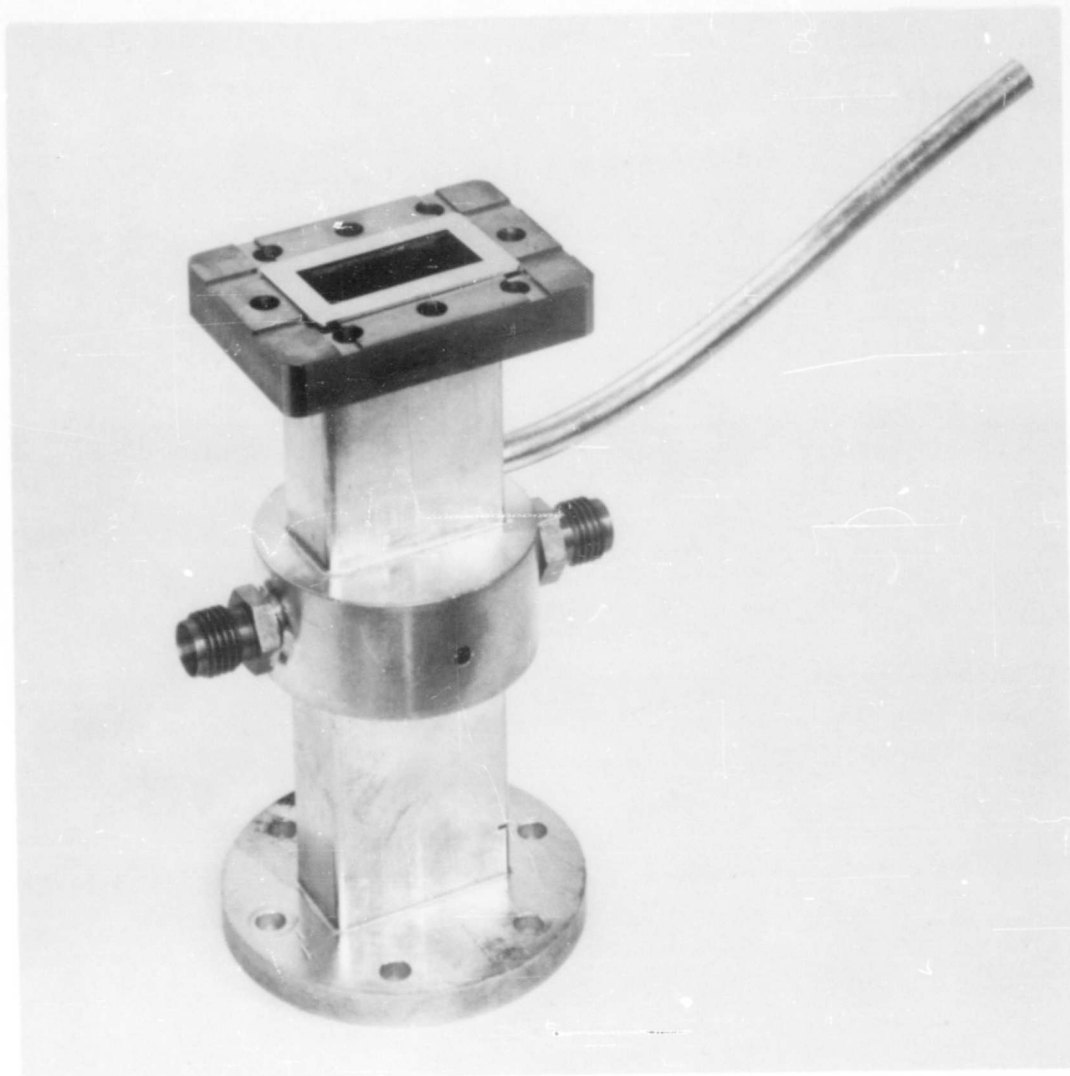


FIGURE 12
SINGLE DISC SAPPHIRE WINDOW ASSEMBLY
USED AS ONE HALF OF WINDOWTRON

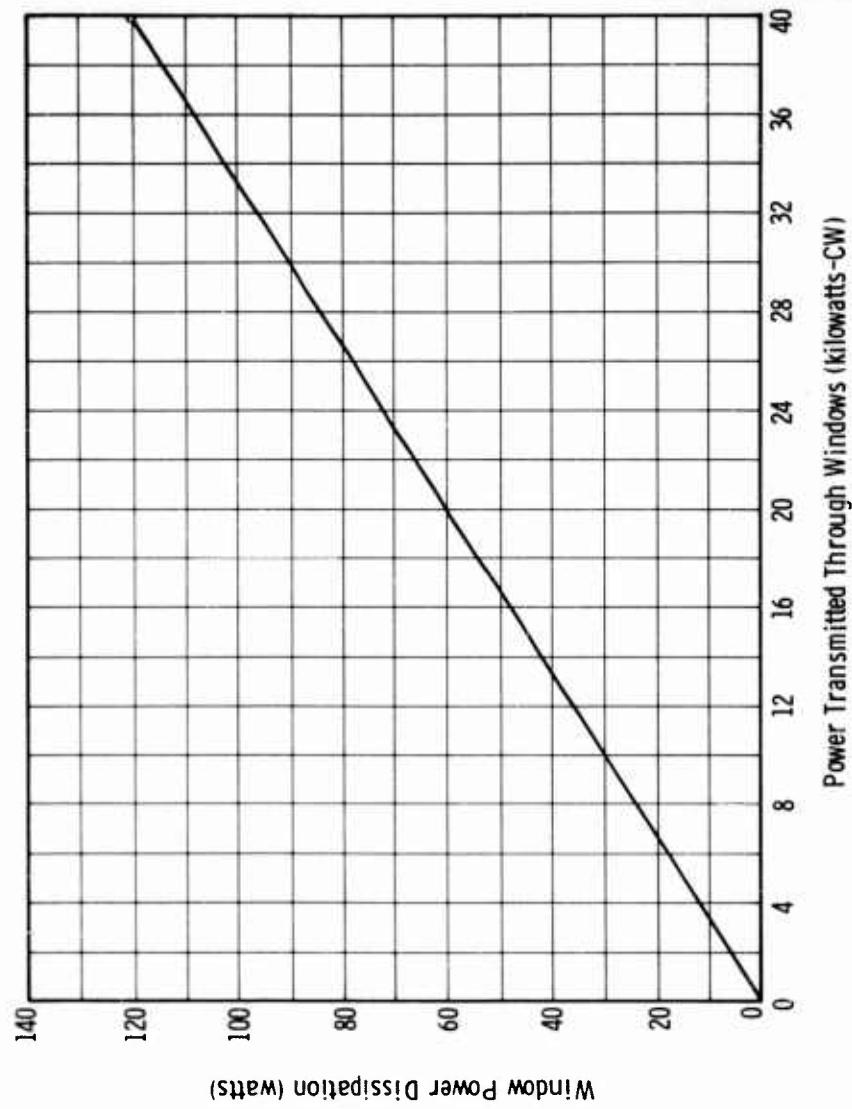


FIGURE 13
AVERAGE DISSIPATION IN SINGLE THIN DISC AL300 WINDOWS

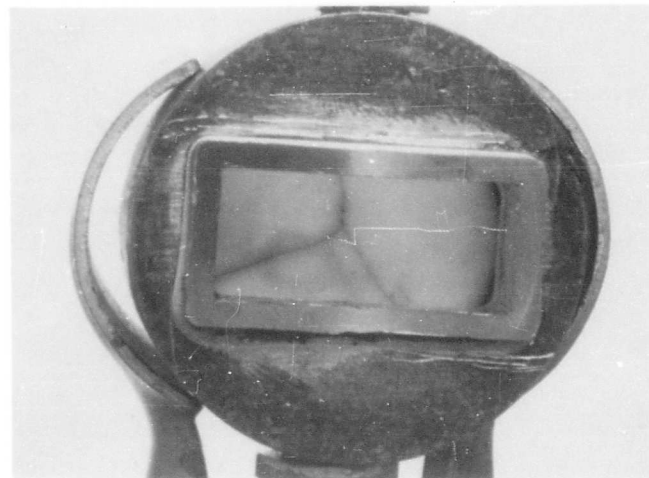
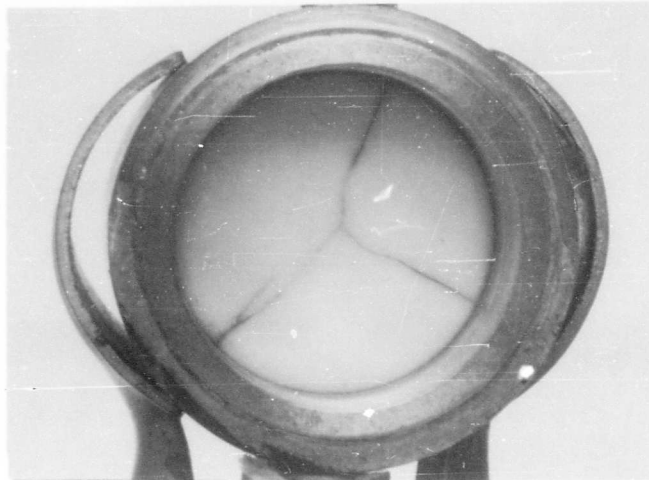


FIGURE 14
ILLUSTRATING RADIAL CRACKS OF FAILURE ON OPPOSITE
SIDES OF A THIN DISC ALUMINA WINDOW

Preliminary work was done in cold testing of several samples of BN and it was found that a good match could be had over a fairly wide bandwidth (Figure 15). With a little more effort it is fairly certain that the bandwidth could be considerably improved. However, work was suspended on this material because high temperature metal-to-boron nitride seals cannot be made reliably.

Boron nitride should not be rejected for this reason. In view of the result of this program, which has shown that high thermal conductivity is essential, BN might yet be an answer to the high average power window problem. Perhaps future work on both the seal technology and high power testing of this material will prove its worth.

4. Fused Quartz Single Discs

Fused quartz or fused silica has repeatedly been considered for use in waveguide windows because of its very low loss tangent which is reported to be 0.0001 or less. Its other properties introduce several disadvantages, some of which assume major importance. In particular, the thermal coefficient of expansion is incompatible with any known metal to which it could be sealed for variable temperature operation. A great deal of effort has been and still is being expended in development of such a seal. For this reason a determined effort was made to establish the actual value of fused quartz as a high average power window.

Once again, the thin disc "poker chip" configuration was used if for no other reason than to give a fair comparison with the alumina and sapphire windows. Because of the quartz-to-metal seal problem, only mechanical pressure seals were made which were vacuum-tight at as high a temperature as 300°C, but opened up at normal bakeout temperatures of 400°C or more. The fact that high temperature vacuum seals were not made on these assemblies in no way altered the validity of pressurized resonant ring testing to establish whether fused quartz does constitute a desirable high power window dielectric. Table III summarizes the pertinent facts concerning the four assemblies tested, and Figure 16 shows the average dissipation measured.

The first two windows failed at 70 and 50 kilowatts, respectively, by melting and actually deforming near the center of the disc as shown in Figures 17 and 18. Cross-sectional photographs (Figure 19) of one of the bubbles was obtained by encasing the disc in a resin and grinding down to the bubble. This bubble appeared to be venting through the disc in the direction of power flow in both cases, leading to the hypothesis that a void or impurity may have caused expansions within the quartz.

TABLE III

SUMMARY OF FUSED QUARTZ HIGH POWER TESTS

Window No.	Max. Power to Which Tested (KW)	Test Conditions and Observations
1	70	Quartz melted near center of disc N ₂ pressure 35 psi both sides GE commercial grade type 101 quartz
2	50	Quartz melted near center of disc N ₂ pressure 35 psi both sides GE commercial grade type 101 quartz
3	120	Quartz became red hot at 100 to 120 kw N ₂ pressure 35 psi both sides Selected bubble-free GE type 101 quartz Red hot quartz ionized nitrogen
4	210	Quartz became red hot at 190 kw N ₂ pressure 35 psi both sides Grade A optical quartz from Amersil Co. No deformation of disc

A bubble-free disc of the same material, GE type 101, was selected to test in window No. 3. Window No. 4 was made with the best optical grade quartz obtainable from the Amersil Co. Both were tested to higher power levels under the same conditions with considerably better results. However, even these two samples became hot enough to glow red hot. Quartz softens at 1670°C and fuses at about 1800°C. It is believed that if these latter two windows had been tested with a vacuum on one side and pressure on the other, the hot areas would have deformed in a way similar to that of the first two.

The results of these four tests, coupled with the excellent results from the sapphire and beryllia windows, led to the conclusion that fused quartz r-f windows would not warrant much attention in the future. Further attempts at their broadbanding or fabrication were halted in favor of channeling maximum effort towards improving other types of windows.

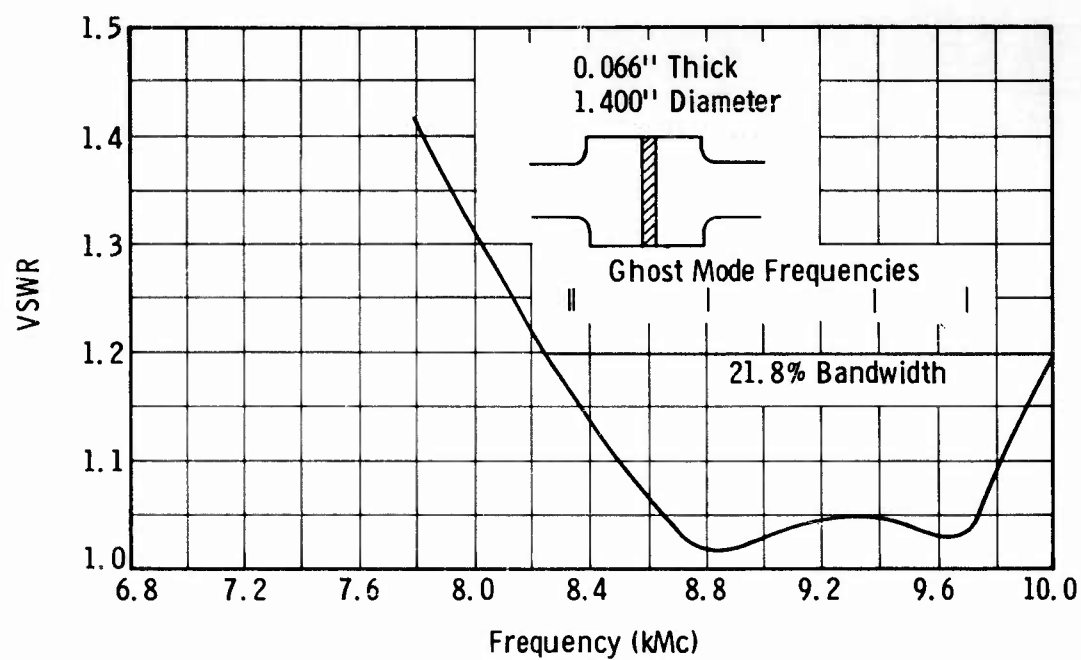


FIGURE 15
SINGLE DISC BORON NITRIDE WINDOW
CHARACTERISTICS VSWR VS FREQUENCY

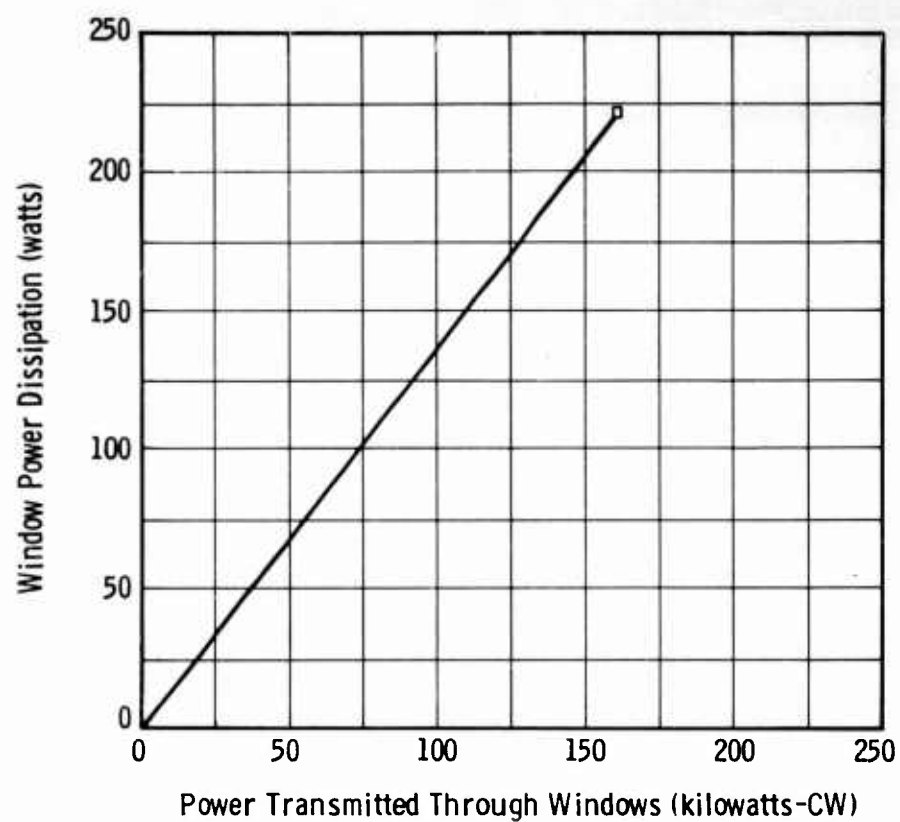


FIGURE 16
AVERAGE DISSIPATION IN THIN DISC FUSED QUARTZ WINDOWS

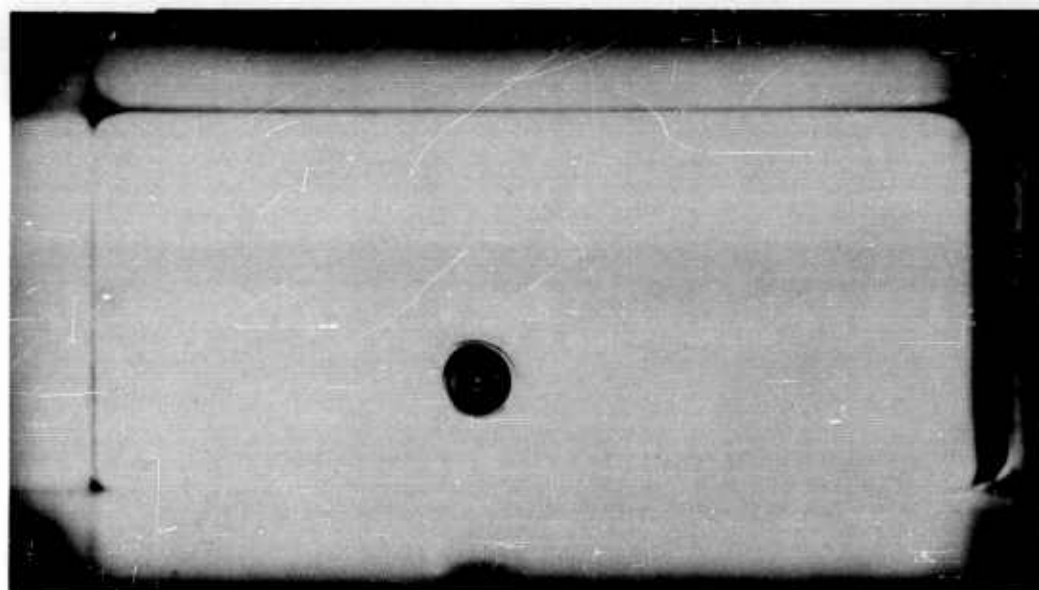


FIGURE 17
FAILURE OF FUSED QUARTZ WINDOW NO. 1

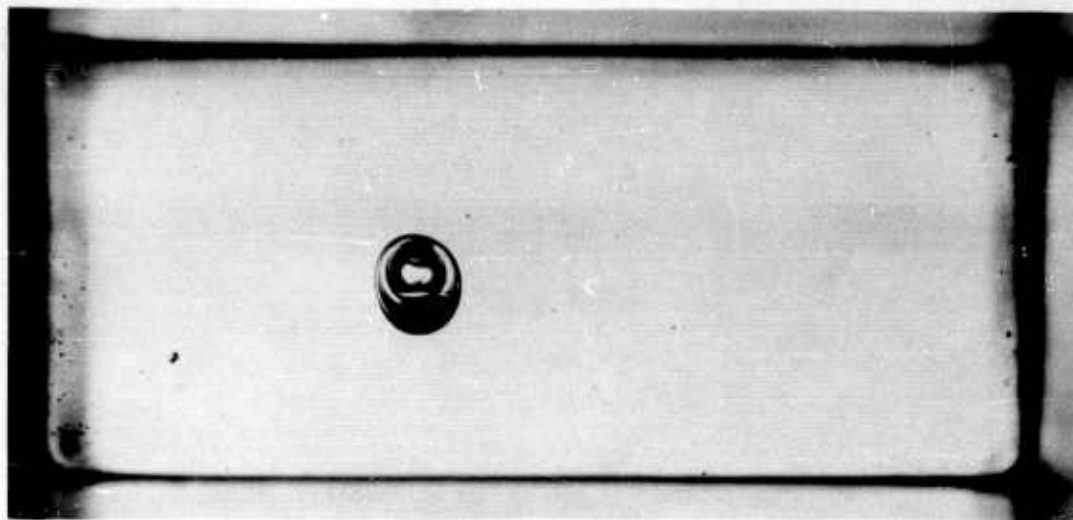
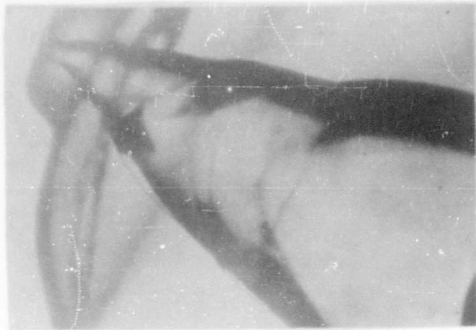


FIGURE 18
FAILURE OF FUSED QUARTZ WINDOW NO. 2



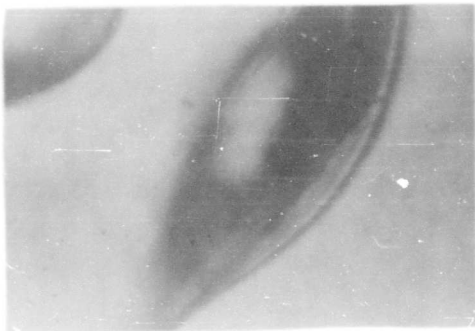
(a)

Cross Section from Window
Center to Power Output Side
Magnification 30 Times



(b)

Cross Section Showing Power
Output Side of Window
Magnification 100 Times



(c)

Cross Section Showing Power
Input Side of Window
Magnification 100 Times

FIGURE 19
CROSS SECTIONS OF R-F MELTED
FUSED QUARTZ BUBBLE

D. Double Thin Disc Windows

1. Temperature Limitations and Cooling Methods

High average power windows using all currently available dielectrics have been shown to dissipate considerable energy as heat even though it may only be a small percentage of the power transmitted through them. With low thermal conductivity paths between the highest power density regions and the nearest heat sink, many windows fail by melting or cracking.

The passage of coolants over these regions suggests fabrication of double thin disc windows in place of single thin disc windows of any configuration. Half-wavelength windows could also be cooled by drilling coolant passages through the blocks. These coolants would be required to pass through r-f propagating regions, placing stringent requirements on their physical properties. High voltage breakdown, specific heat, dielectric constant, loss tangent, viscosity and compatibility with other materials are the more important ones. Most coolants available, either fluid or gaseous are disqualified for lack of one or more of these properties.

Inert fluorocarbon liquids such as FC-75* and FC-43* do qualify in most respects, with the possible exception of having rather high loss tangents. These are 0.009 and 0.0036, respectively, at 8.5 Gc. The possibility of using the freons, air or nitrogen as cooling was also considered.

2. Fluid Cooled Double Discs

Using the results of preliminary tests, coupled with an analysis of the available equipment and time, the decision was made to concentrate on cooling windows with FC-75 and with dry nitrogen. The cost of FC-75 is \$138 per gallon or about half that of FC-43. So a savings was realized. The higher loss tangent of FC-75 could also be turned into an advantage.

High Q ghost and trapped modes exist in all windows and are responsible, among other things, for the dissipation of much r-f energy as heat and fracture of windows. Damping these modes is possible in a lossy dielectric provided the heat can be carried away conveniently. The lossy FC-75 fluid provides just such a condition and it was shown that indeed the spurious modes were damped to an undetectable level in a double disc window when the space between discs was wide enough. The minimum width of spacing required to accomplish this was found to be 0.060 to 0.080 inch.

- - - - -
* Trade name for 3M Company inert fluorochemicals.

A fairly accurate estimate of the losses to be expected in this type of window can be made using Equation 1.

$$P_{\text{lost}} = P_{\text{in}} (1 - e^{-2\alpha\ell}) \quad (1)$$

where

$$\alpha = \frac{k}{2} \frac{\epsilon''}{\epsilon' \sqrt{1 - (f_c/f)^2}}$$

$$k = \frac{2\pi}{\lambda_0} \sqrt{\epsilon'}$$

$$f_c = \frac{0.293c}{a \sqrt{\epsilon'}}$$

A series expansion of $e^{-2\alpha\ell}$ gives the approximation

$$P_{\text{lost}} \cong 2\alpha P_{\text{in}} \ell \quad (2)$$

which can be shown to be correct within 0.25 per cent for the range of losses under discussion.

Solving Equation (2) with:

$$P_{\text{in}} = 100 \text{ Kw}$$

$$\ell = 0.080 \text{ inch}$$

$$\frac{\epsilon''}{\epsilon'} = .009$$

$$\epsilon' = 1.80$$

$$f = 8.5 \text{ Gc}$$

$$a = 0.660 \text{ inch cylinder radius}$$

then

$$P_{\text{lost}} = 492 \text{ watts}$$

It was shown in the discussion on the single disc alumina windows that the loss in that window was very close to 3 watts per kilowatt. At 100 kilowatts this represents 300 watts dissipated power which is a composite of ceramic, seal and wall losses in the vicinity of the window. Assuming a similar magnitude of losses will occur in the double disc window, the total loss at 100 kilowatts in a double disc window is then estimated to be about 800 watts.

Reference to Figure 20 will show that the estimate is very close to the actual measured losses for window Nos. 3, 4 and 7. Estimated losses for window No. 5 are 546 watts at 100 kilowatts or almost exactly what was measured. This latter window had only 0.040 inch between the discs. Table IV summarizes the test powers, dimensions and type of failure experienced.

Window No. 3 was the only double disc fluid cooled window that failed at or below 170 kilowatts. The dissipation curve (Figure 20) indicates that a great deal more heating was taking place in the window than in any of the others, and the photograph (Figure 21) of the failure showed that the ceramic had actually melted through on the power output side. The only explanation that can be offered is that the ceramic contained a flaw causing failure before the power input disc was damaged. The input window still tested vacuum-tight after the experiment.

As discussed in the first Quarterly Technical Note,¹ the cross-section of the cooling fluid vents into the region between the discs was kept to a minimum to prevent the interruption of wall currents. As a result, fluid flow was limited. During the high power tests on all of the fluid cooled windows the FC-75 became agitated because of boiling at the 120 to 150 kilowatt levels, becoming more agitated as power was increased. Of course, this affected the match in the window, which in turn caused the power in the ring to oscillate rapidly over a small power range. This would undoubtedly be a factor in promoting earlier than necessary failure of this window design.

Figure 22 is a photograph of the actual cross-sections of two double disc windows showing the spacing between the discs as well as the single fluid input and output vents. A higher fluid flow with less pressure would be obtained by increasing the number of these vents. With sufficient flow, boiling of the FC-75 would be eliminated. These tests and results indicate that more work along these lines should be done.

To verify further the encouraging promises of high power fluid cooled windows, two of the windows already tested to 160 and 150 kilowatts without failure were retested without cooling of any kind except air convection and conduction through the connecting waveguides. These were double disc windows No. 4 and No. 5, and both failed at 20 kilowatts with vacuum on one side and pressurized to 30 psi dry nitrogen on the other. This is conclusive proof that a less than 20 kilowatt window will become a perfectly good 160 kilowatt (or more) window with the addition of cooling,

TABLE IV

SUMMARY OF HIGH POWER TEST ON DOUBLE THIN DISC FC-75 COOLED WINDOWS

<u>Window Number</u>	<u>Maximum Test Power (KW)</u>	<u>Specifications and Test Conditions</u>
1	0	Al300 Discs - .025 thick - mechanical failure due to excessive pressure.
2	180	Al400 Discs - .030 thick - .080 between discs - 32 psi nitrogen pressure both faces - power input window failed by cracking.
3	90	Al400 Discs - .035 thick - .80 between discs - vacuum one side in test - failed at power output side by melting.
4	160	Al400 Discs - .035 thick - .080 between discs - vacuum one side in test - no failure - drive power limited-without FC-75 cooling both discs failed at 20 kw.
5	150	Al300 Discs - .030 thick - .040 between discs-vacuum one side in test - no failure - drive power limited - without cooling both discs failed at 20 kw.
6	0	Al400 Discs - .034 thick - .080 space between discs - no high power test.
7	170	Al400 Discs - .034 thick - .080 space between discs - vacuum one side in test - input window failed by cracking.
8	0	Al300 Discs - .030 thick - .080 space between discs - seal failed in pressure test.

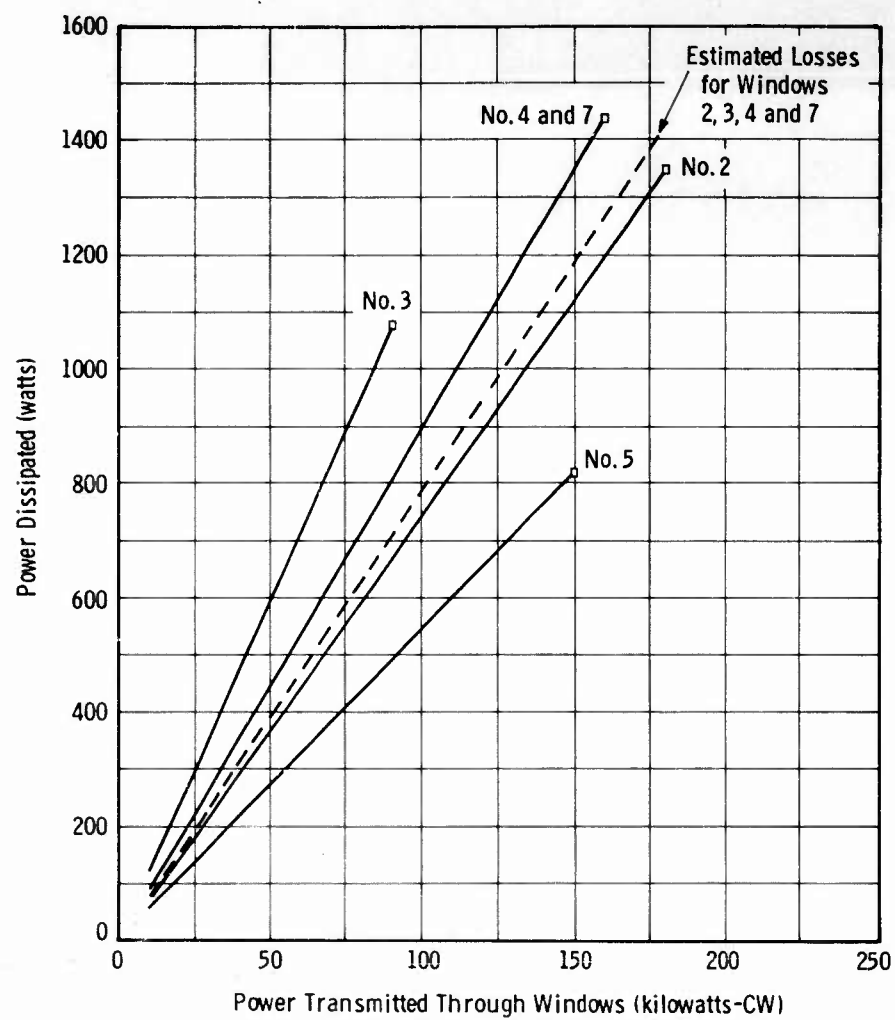


FIGURE 20
POWER DISSIPATION IN VARIOUS DOUBLE DISC FC-75
COOLED WINDOW ASSEMBLIES

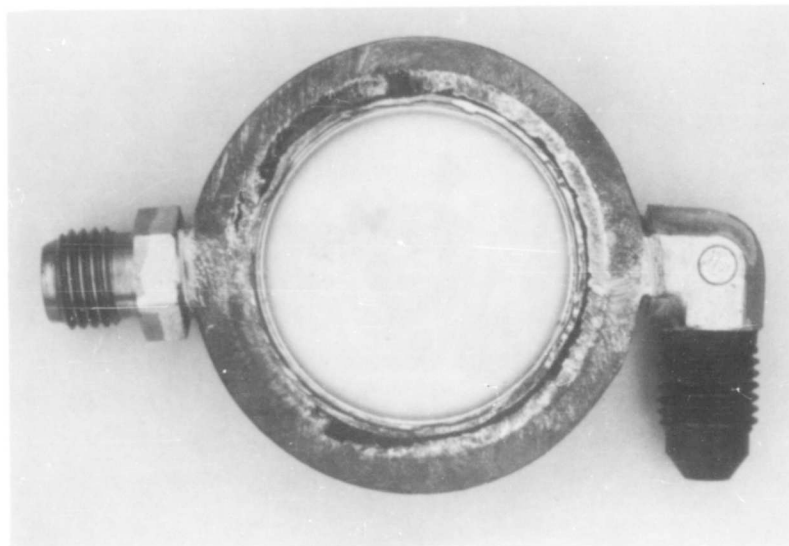
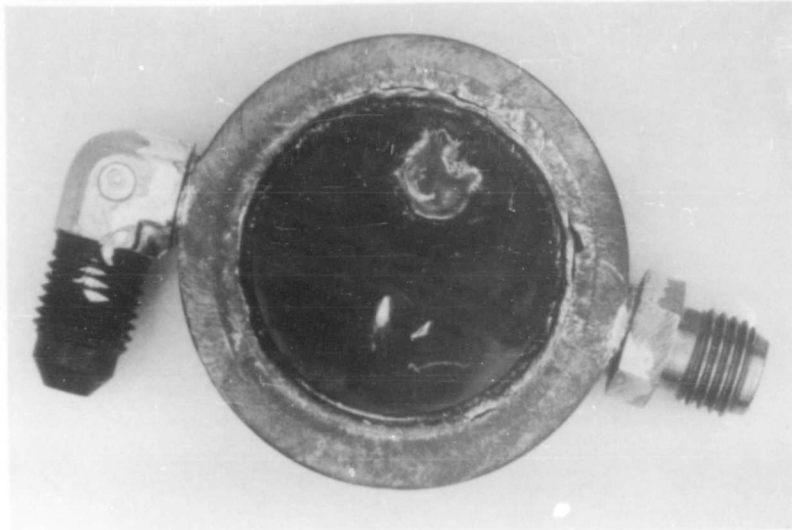
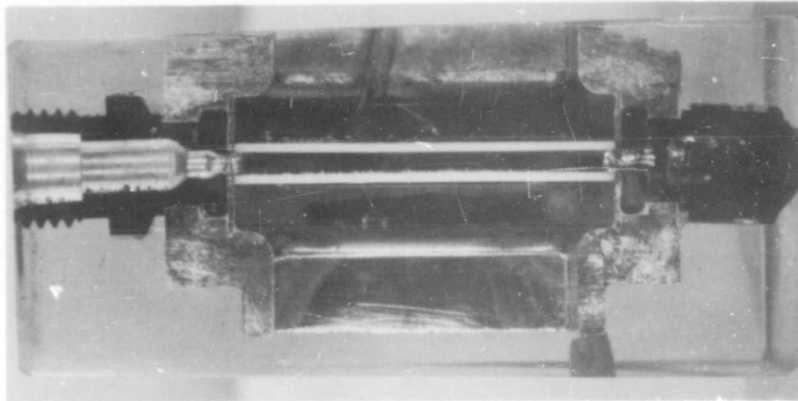
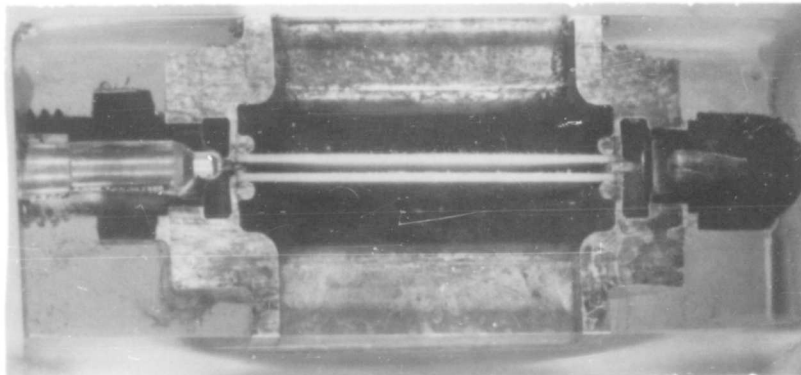


FIGURE 21
DISASSEMBLED FC75 COOLED WINDOW SHOWING HIGH
TEMPERATURE FAILURE (PRESSURIZED SIDE FAILED)



(a) AL400 Double Disc Window No. 7



(b) AL300 Double Disc Window No. 8

FIGURE 22
CROSS-SECTIONS OF DOUBLE DISC WINDOWS

even though the cooling were inadequate. It is further concluded that a double disc sapphire window cooled with FC-75 would make an exceedingly high average power window having a very wide band.

All of the double disc fluid cooled windows fabricated had bandwidths in excess of 25 per cent.^{1, 2} A photograph of a completed test model is shown in Figure 23.

3. Gas Cooled Double Discs

A sketch of another double disc window configuration is shown in Figure 24 along with its VSWR characteristics. Several differences become apparent on close inspection. Conical tapers are used to reduce the excitation of evanescent modes in the region of the transitions from the TE_{10} to the TE_{11}^0 modes. The ceramic discs are mounted at an electrical field minimum because the cylinder is electrically near one wavelength long. Each window thickness is fully as thick as for a single disc window. An additional hoop support is provided not only for strength but for exact positioning of the discs in the brazing operations.

As a result of the above innovations, the bandwidth of the finished assemblies was reduced to 9.5 per cent. For many applications such a bandwidth would be more than adequate. A photograph of the finished assembly as well as a cross-sectional sketch are shown in Figure 25. Two such assemblies were built and tested vacuum-tight before high power tests were made.

Two completely independent cooling systems were built into this window. Copper losses as well as conducted ceramic losses were removed by water flow and monitored continuously by calorimetric means. The other two vents provided an independent system for separately cooling the inside faces of the window by a gas, which in this case was dry nitrogen.

Both windows failed at exactly the same power levels, 100 kilowatt. At failure, No. 1 window had no gas cooling but was adequately cooled with water around its cylindrical cavity. Both discs failed simultaneously by fracture and melting near the center of the discs (see Figure 26). Only the disc on the power input side (vacuum side) of window No. 2 failed. The differences in water jacket heat flow with and without gas cooling are shown in Figure 27. The effect of the gas cooling is definitely measureable, but shows only about a 12 per cent improvement.

The full-wavelength long, double disc, conical transition window described in this section out-performed the half-wavelength, single disc, abrupt transition window by a factor of 2.5 to 3, and equaled the power capacity of the half-wavelength block alumina windows. The main reason for this is the removal of the transitions from such close proximity to the ceramics. Replacement of the

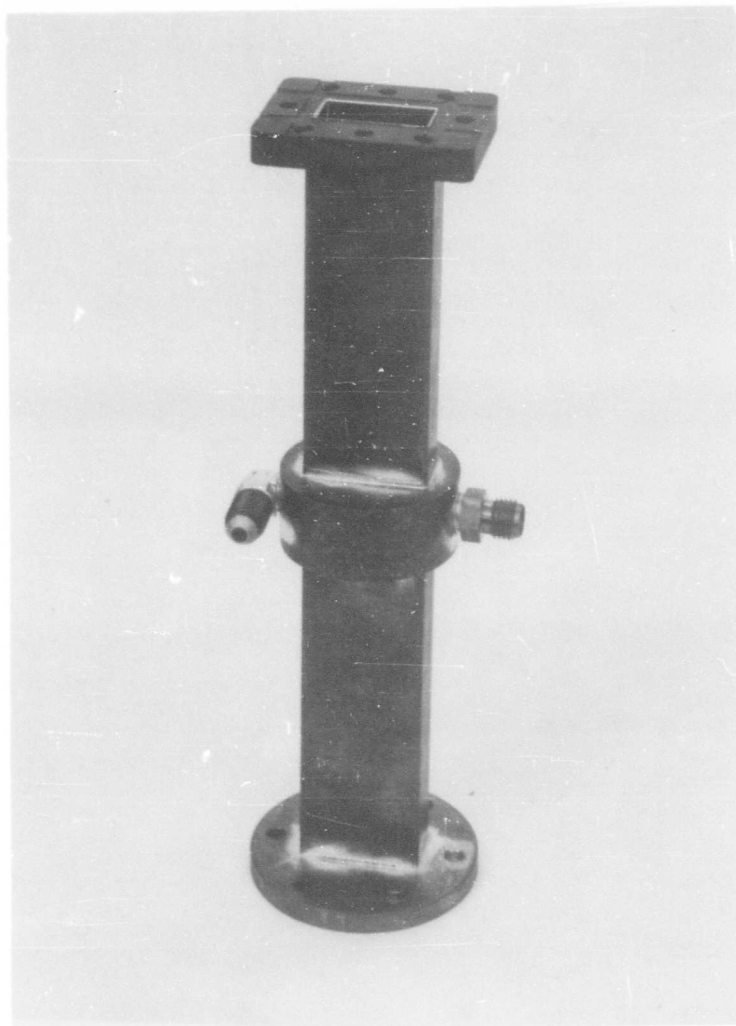


FIGURE 23
HIGH POWER FC-75 COOLED DOUBLE DISC WINDOW

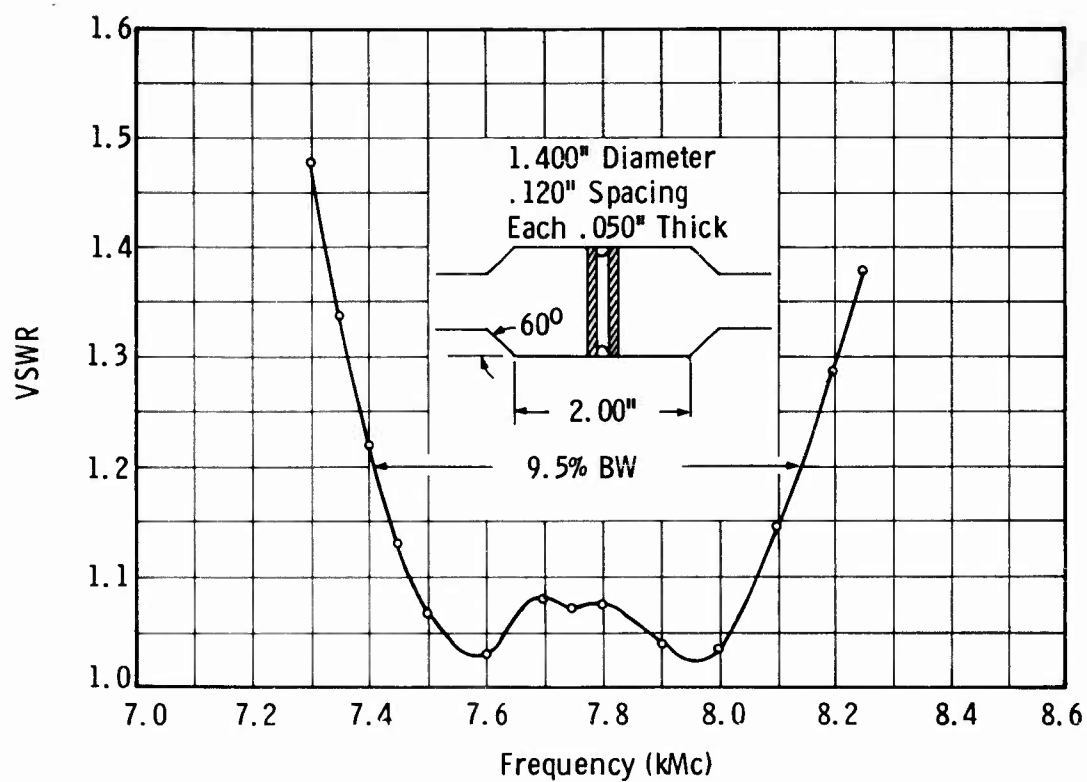
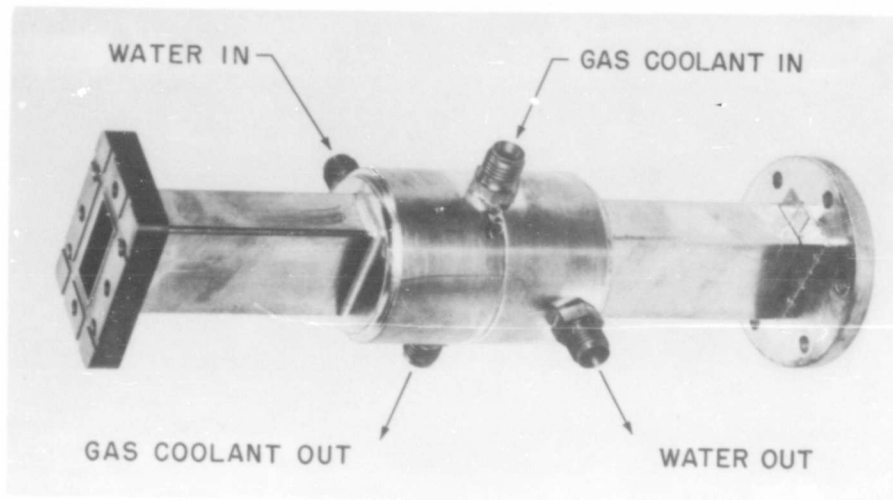
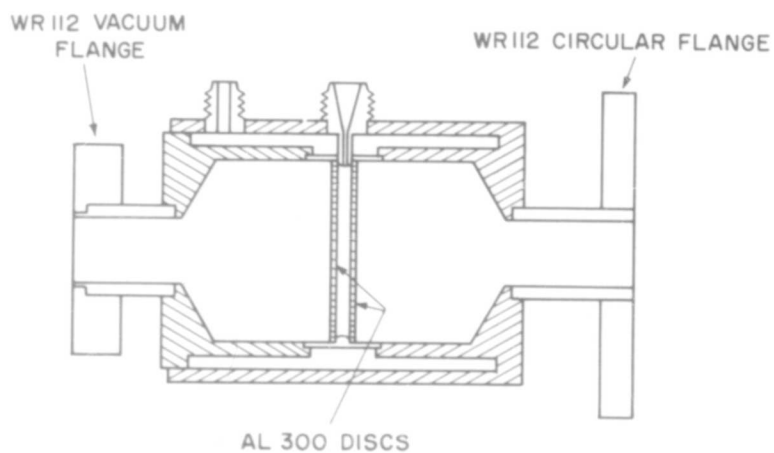


FIGURE 24
VSWR CHARACTERISTICS OF A DOUBLE DISC AL300
WINDOW WITH CONICAL TRANSITIONS



(a) Final Assembly



(b) Full Scale Cross-Sectional Sketch

FIGURE 25
DOUBLE DISC AL300 WINDOW ASSEMBLY

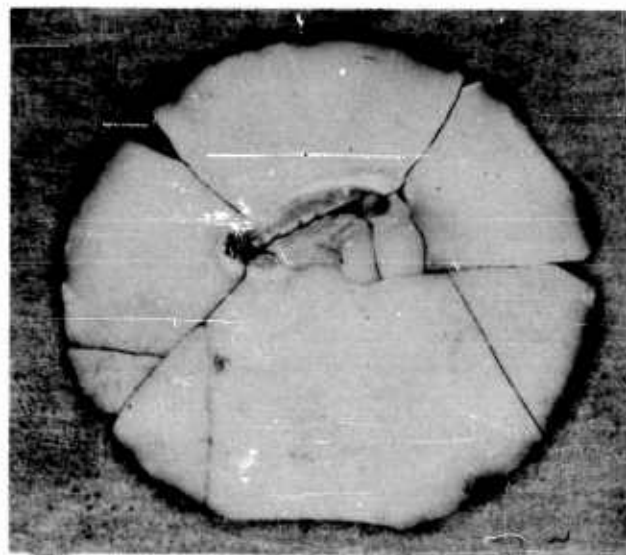
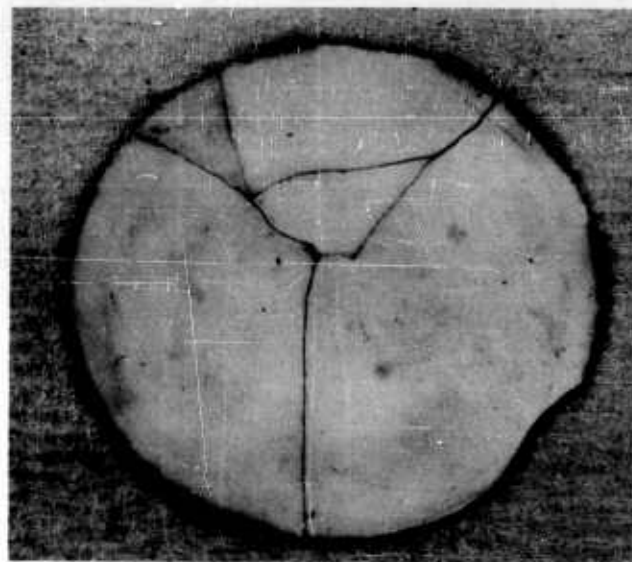


FIGURE 26
DISASSEMBLED DOUBLE DISC WINDOW NO. 1 CERAMICS
SHOWING HIGH TEMPERATURE FAILURE

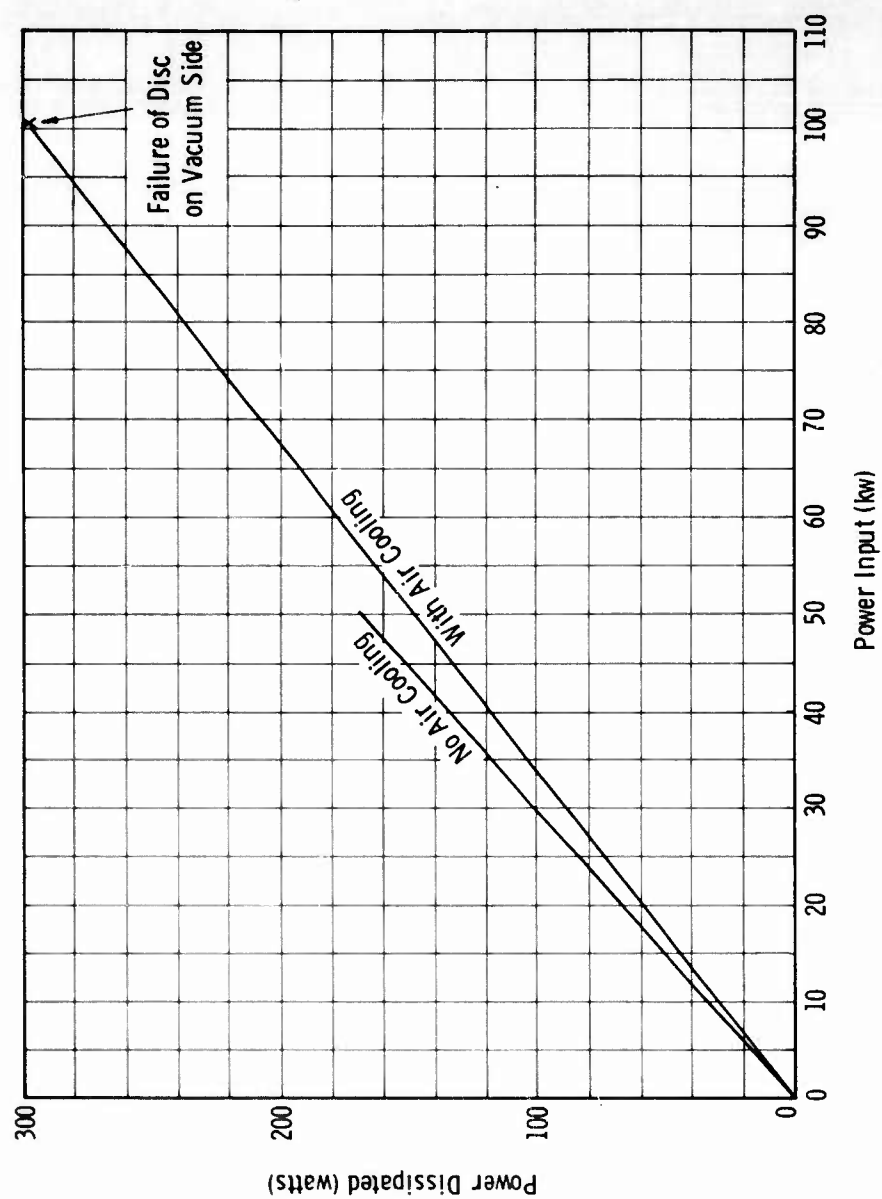


FIGURE 27
POWER DISSIPATION IN DOUBLE DISC AL300 WINDOW
WITH AND WITHOUT DRY NITROGEN COOLING

alumina discs by a high strength material such as sapphire or by a high thermal conductivity material such as beryllia would certainly make this window compete very seriously with the best windows tested in this program.

2-2. WINDOW DESIGN

A. Broad Banding of Half-Wavelength Blocks - Impedance Match and Mode Freedom

Perhaps one of the biggest problems encountered in the selection of a self-resonant block window size is the frequency at which ghost modes will exist and how to prevent their excitation or entrance into the frequency band of interest. As previously reported,¹ the ghost modes can be determined very accurately for any given block window by means of a programmed solution for derived mode equations. Two such mode plots are shown in Figures 28 and 29, both of which are for blocks self-resonant at 8.0 Gc. With a normal aspect ratio, the alumina window would have no mode freedom whatsoever where the beryllia window would have approximately a 9 per cent mode free bandwidth. Juggling of the aspect ratio would be one way of increasing this bandwidth. Another way is cutting the block for self-resonance somewhere away from the center of the desired band. As will be shown, this cannot be carried too far or impedance matching will not be possible.

Once a block has been selected to fill the requirements of a given application, the problem of broadbanding the window must be faced. This subject has been covered by this program's Quarterly Technical Note No. 3,³ and by others, such as Churchill.⁶ With the use of filter networks, block windows can be matched over a typical bandwidth of 20 per cent with little or no difficulty. For example, a specification for 10 per cent bandwidth window (say 7.6 to 8.4 Gc) would allow the block to be cut for resonance at any frequency between 7.6 and 8.4 Gc. If cut at 8.4 Gc the 20 per cent matched bandwidth would be approximately 7.6 to 9.0 Gc or wide enough to satisfy the requirements of the example. By these techniques a window can be designed mode free and well matched over a reasonable range of frequencies. It is not anticipated that mode free bandwidths will exceed 12 per cent with normal aspect ratios. Half height guides would be considerably better in this respect, but then power handling capacity is substantially reduced. A compromise must then be made between maximum bandwidth and maximum power handling capacity.

B. Window Synthesis

Another method of broadbanding waveguide windows, other than the rather tedious Smith plotting method, is by synthesis of the entire window. This can be done even before the first piece of ceramic is purchased. In general, there are two types of configurations which will be built and which can be analytically synthesized. These are the self-resonant block and the thin disc windows, or any variations thereof. Figure 30 illustrates models of these two configurations. Simpler models could have been

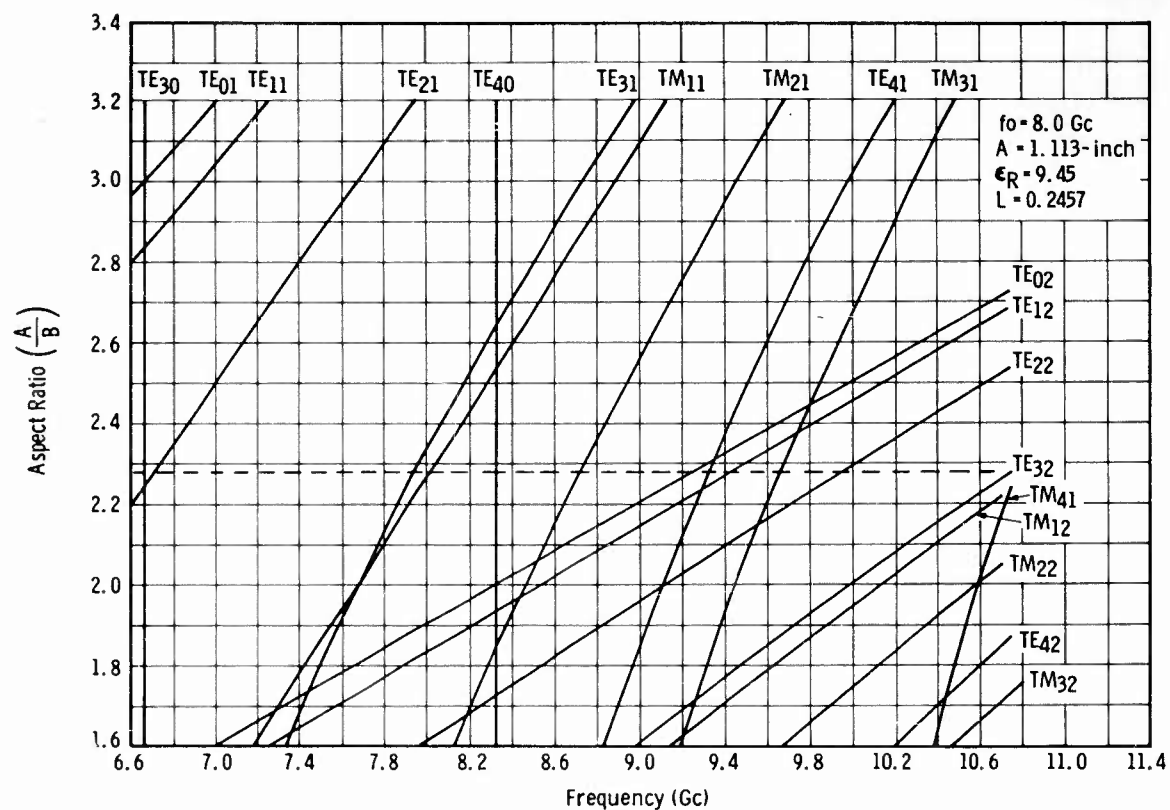


FIGURE 28
MODE FREQUENCY PLOT FOR AL300 BLOCK WINDOWS

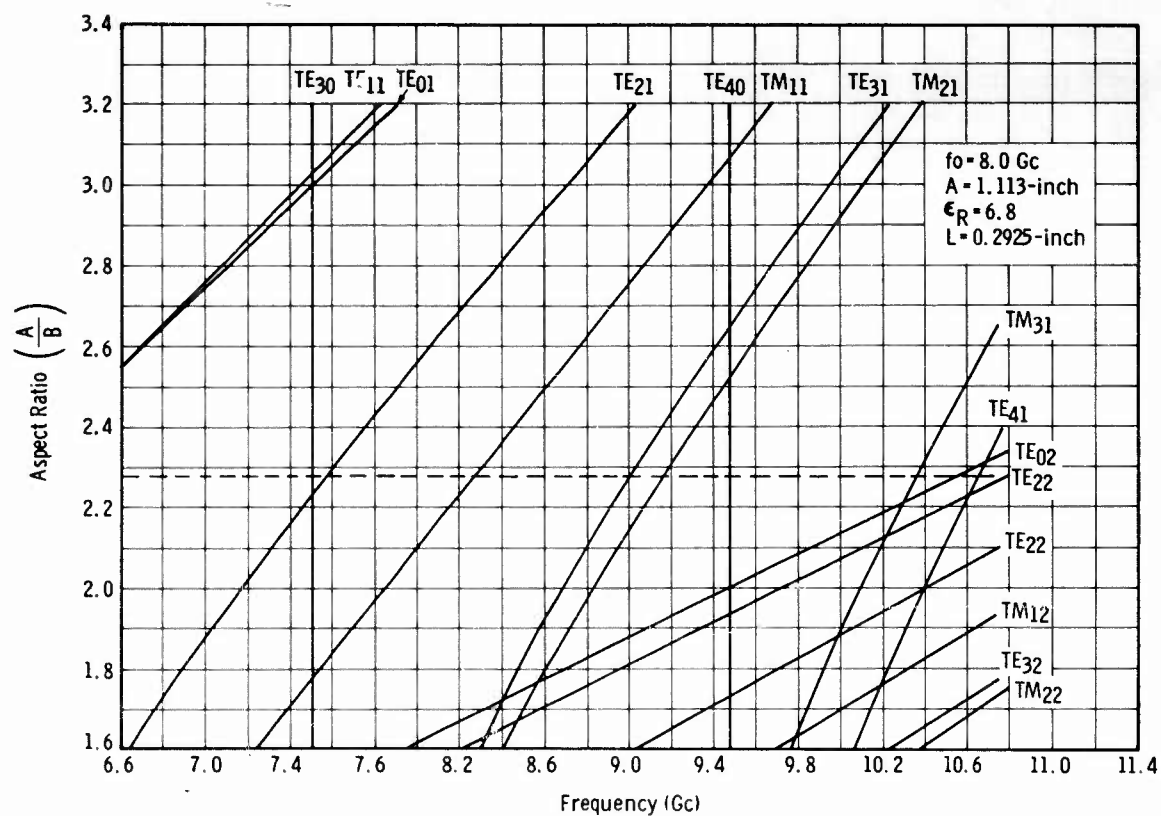
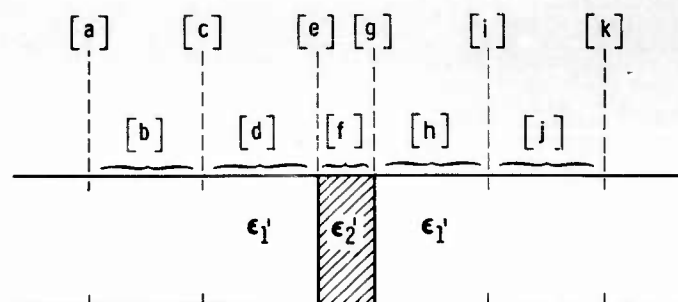
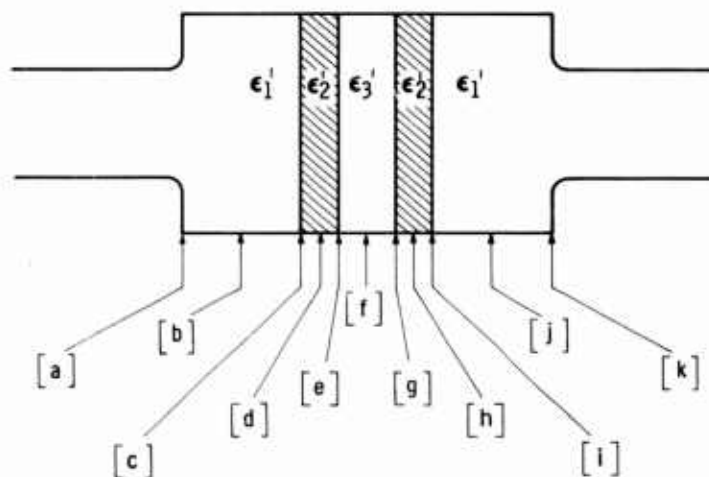


FIGURE 29
MODE FREQUENCY PLOT FOR BERYLLIA BLOCK WINDOW



(a) Half Wavelength Block Window With Cascaded Broadbanding Irises



(b) Disc Type Window With Dielectric Cooling

FIGURE 30
WINDOW CONFIGURATION MODELS SHOWING CONTRIBUTIONS
OF MATRIX COMPONENTS [a] THROUGH [k]

chosen for the following analysis, but then the solution would be limited if the need arose for more complicated cases. Both models have contributions from eleven complete and distinct sources requiring analytic expressions for each one. In most cases these circuit components will be limited to irises, lengths of waveguide (dielectric or air loaded), dielectric interfaces and transitions from one size of waveguide to another.

Transmission parameters⁷ are used to define these components. For example, there are eleven component matrices in each of the models of Figure 30. These are lettered consecutively from [a] to [k], although each matrix in the block window does not necessarily have the same meaning as its counterpart in the disc window. To avoid confusion, each model will be discussed independently.

1. Half-Wavelength Block Window Circuit Components

Matrixes [a], [c], [i] and [k] can be identified as inductive irises placed at intervals along the waveguide. An analytic expression can be written^{8,9} for the shunt susceptance of inductive irises and is:

$$\frac{B}{Y_0} = -j \frac{\lambda_g}{a} \cot^2 \frac{\pi d}{2a} \left\{ 1 + \frac{3}{4} \left[\frac{1}{\sqrt{1 - \left(\frac{2a}{3\lambda_0}\right)^2}} - 1 \right] \sin^2 \frac{\pi d}{a} \right\}^{-1}$$

where

- λ_g = waveguide wavelength
- λ_0 = free space wavelength
- a = waveguide width
- d = distance separating inside edge of iris pair

The transmission parameter matrices are then defined as,

$$T = \begin{bmatrix} 1 - \frac{B}{2Y_0} & -\frac{B}{2Y_0} \\ \frac{B}{2Y_0} & 1 + \frac{B}{2Y_0} \end{bmatrix}, \text{ for inductive irises.}$$

Matrixes [b], [d], [f], [h] and [j] are identifiable as sections of connecting waveguide. This is true whether they are air or dielectric filled. A general expression for the transmission parameter matrix is

$$T = \begin{bmatrix} e^{-j\beta L} & 0 \\ 0 & e^{j\beta L} \end{bmatrix}$$

$$= \begin{bmatrix} \cos \beta L - j \sin \beta L & 0 \\ 0 & \cos \beta L + j \sin \beta L \end{bmatrix}$$

Where

$$\beta = \omega \sqrt{\mu \epsilon} \left[1 - (f_c/f)^2 \right]^{1/2}$$

$$\epsilon = \epsilon_0 \epsilon^1$$

ϵ_0 = dielectric constant of free space

ϵ^1 = Relative dielectric constant.

The cutoff wavelength for rectangular guides, such as used in the rectangular block window under discussion, is

$$(fc)_{m,n} = \frac{1}{2\sqrt{\mu\epsilon}} \sqrt{\left(\frac{m}{a}\right)^2 + \left(\frac{n}{b}\right)^2} \text{ which reduces to}$$

$$fc = \frac{1}{2a\sqrt{\mu\epsilon}} \text{ for the TE}_{10}^{\square} \text{ mode. } a = \text{waveguide broad dimension}$$

The integers m and n denote the half sine variations in the X and Y coordinate directions of rectangular waveguide.

Therefore

$$\beta = \frac{2\pi}{\lambda_0} \left[\epsilon^1 - \left(\frac{\lambda_0}{2a}\right)^2 \right]^{1/2} \text{ for the TE}_{10}^{\square} \text{ mode.}$$

The remaining two matrices for the block window are from the contributions of the dielectric interfaces. These have been shown³ to be

$$T = \begin{bmatrix} \frac{1+R}{2} & \frac{1-R}{2} \\ \frac{1-R}{2} & \frac{1+R}{2} \end{bmatrix}$$

Where

$$R = \frac{Z_{01}}{Z_{02}}$$

Z_{01} = Characteristic impedance on the input side of the interface.
 Z_{02} = Characteristic impedance on the output side of the interface.

Therefore

$$R_1 = \frac{Z_{01}}{Z_{02}} = \left[\frac{\epsilon_2^1 - \left(\frac{\lambda_0}{2a}\right)^2}{\epsilon_1^1 - \left(\frac{\lambda_0}{2a}\right)^2} \right]^{1/2} \quad (\text{TE}_{10} \text{ modes})$$

for the first interface at [e]. For the second interface at [g]

$$R_2 = \frac{1}{R_1}$$

so

$$R_2 = \left[\frac{\epsilon_1^1 - \left(\frac{\lambda_0}{2a}\right)^2}{\epsilon_2^1 - \left(\frac{\lambda_0}{2a}\right)^2} \right]^{1/2}$$

These definitions completely specify the component parts of the half-wavelength block window. How they can be used will be discussed immediately following the definitions of the components for the window of Figure 30 (b).

2. Dielectric Cooled Disc Window Circuit Components

The definition for the matrices

[b], [d], [f], [h] and [j]

is identical to that given for the rectangular block or

$$T = \begin{bmatrix} \cos \beta L - j \sin \beta L & 0 \\ 0 & \cos \beta L + j \sin \beta L \end{bmatrix}$$

The difference is that now the waveguide being considered is cylindrical in shape and is propagating the TE_{11}^0 mode. From⁷

$$fc \left(TE_{n1} \right) = \frac{P_{n1}^1}{2\pi r \sqrt{\mu\epsilon}}$$

the specific cutoff frequency for the TE_{11}^0 mode is $fc = \frac{0.29306}{r \sqrt{\mu\epsilon}}$

Therefore

$$\beta = \frac{2\pi}{\lambda_0} \left[\epsilon^1 - \left(\frac{0.29306 \lambda_0}{r} \right)^2 \right]^{1/2} \quad \text{for } TE_{11}^0 \text{ modes}$$

r = cylindrical waveguide radius

ϵ^1 = the specific relative dielectric constant in each section of waveguide

The general definition of the dielectric interface components remains the same; however, for the double disc window the number of interfaces is also doubled. The dielectric constant of the coolant must also be taken into consideration. At interface [c] in circular guide

$$R_1 = \frac{Z_{01}}{Z_{02}} = \left[\frac{\epsilon_2^1 - \left(\frac{0.29306 \lambda_0}{r} \right)^2}{\epsilon_1^1 - \left(\frac{0.29306 \lambda_0}{r} \right)^2} \right]^{1/2}$$

at [e] ,

$$R_2 = \frac{Z_{02}}{Z_{03}} = \left[\frac{\epsilon_3^1 - \left(\frac{0.29306 \lambda_0}{r} \right)^2}{\epsilon_2^1 - \left(\frac{0.29306 \lambda_0}{r} \right)^2} \right]^{1/2}$$

at [g] ,

$$R_3 = \frac{1}{R_2}$$

at [i] ,

$$R_4 = \frac{1}{R_1}$$

These are then inserted into

$$T = \begin{bmatrix} \frac{1+R}{2} & \frac{1-R}{2} \\ \frac{1-R}{2} & \frac{1+R}{2} \end{bmatrix}$$

in the proper order.

The first and last transmission parameter matrices, $[a]$ and $[k]$, cannot be specified without laboratory measurement. Abrupt irregular discontinuities in waveguide sections or abrupt transitions from one size and type of waveguide to another, such as that used in the Symons-type window, can be measured fairly accurately.¹⁰ Very briefly, this method consists of measuring the VSWR and position of voltage minimum with a slotted line by looking through the discontinuity at a short circuit. The short is varied with the frequency fixed over $\lambda g/2$ in several equal increments. These data are then used to calculate phase angles which are plotted on polar coordinate graph paper along with the magnitudes given by the VSWR measurements. The magnitude and phase of the scattering matrix coefficients S_{11} , S_{12} and S_{22} are determined from these plots.

The scattering coefficients for a 1.400-inch diameter to WR112 waveguide abrupt transition are shown in Figure 31. These were measured using the techniques outlined above.

Once the scattering coefficients have been determined the transmission parameters can be specified³ as

$$T = \begin{bmatrix} S_{12} - \frac{S_{11}S_{22}}{S_{12}} & \frac{S_{22}}{S_{12}} \\ -\frac{S_{11}}{S_{22}} & \frac{1}{S_{12}} \end{bmatrix}$$

If $[a]$ is measured, $[a]$ and $[k]$ are related by

$$\begin{aligned} a_{11} &= k_{11} \\ a_{12} &= -k_{21} \\ a_{21} &= -k_{12} \\ a_{22} &= k_{22} \end{aligned}$$

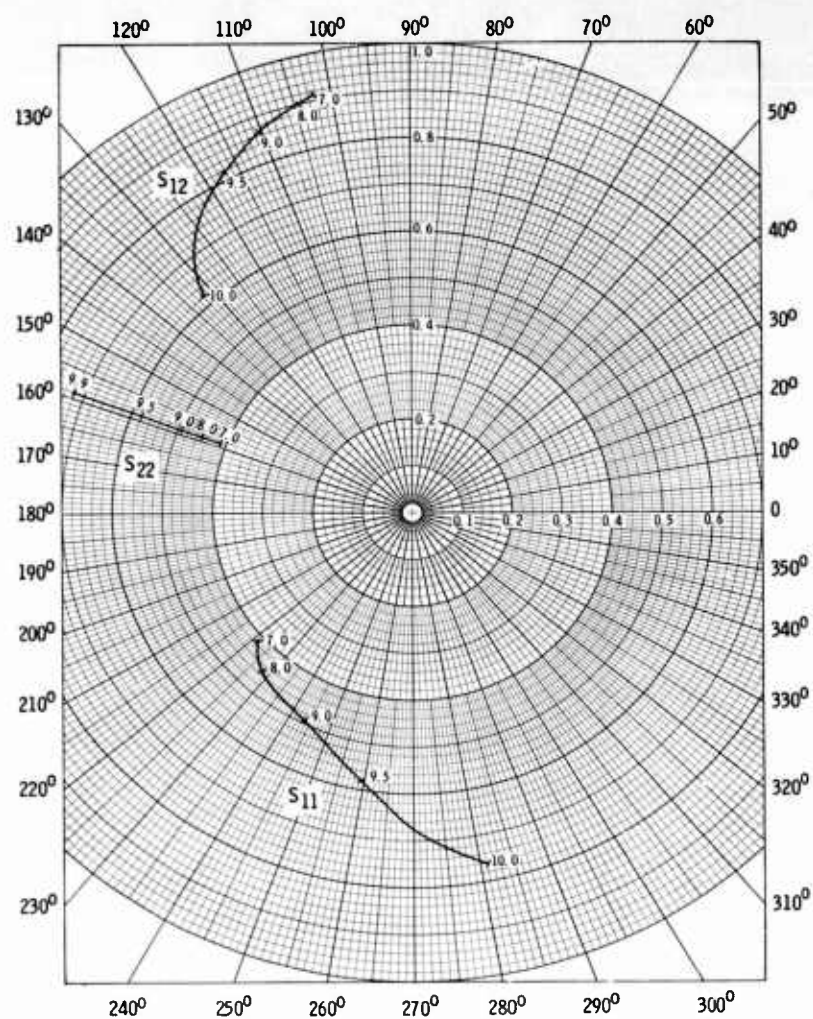


FIGURE 31
SCATTERING MATRIX COEFFICIENT VALUES FOR 1.4-INCH
DIAMETER TO WR12 WAVEGUIDE TRANSITION

3. Computation of Waveguide Window Characteristics

With the above waveguide window circuit components specified by equations or measurements a product of all of them in a cascaded network will give a resulting matrix $[T]$.

That is $[T] = [a] [b] [c] \dots [i] [j] [k]$

where

$$[T] = \begin{bmatrix} T_{11} & T_{12} \\ T_{21} & T_{22} \end{bmatrix}, \quad [a] = \begin{bmatrix} a_{11} & a_{12} \\ a_{21} & a_{22} \end{bmatrix} \quad \text{etc.}$$

The composite window can be represented as shown in Figure 32.

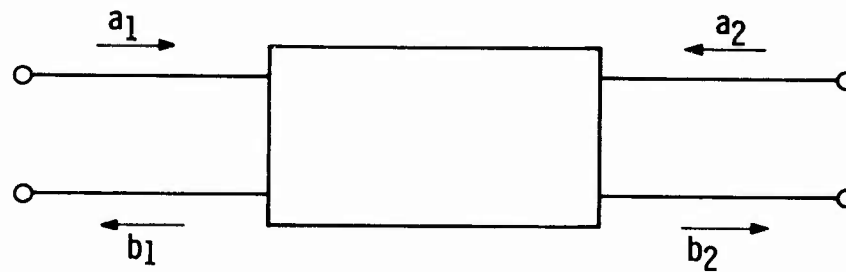


FIGURE 32
FOUR TERMINAL NETWORK REPRESENTATION
OF A WAVEGUIDE WINDOW

It has been demonstrated³ that

$$\begin{aligned} b_2 &= T_{11} a_1 + T_{12} b_1 \\ a_2 &= T_{21} a_1 + T_{22} b_1 \end{aligned}$$

where

a_1 is the incident wave at the input

b_1 is the reflected wave at the input

a_2 is the incident wave at the output

b_2 is the reflected wave at the output

If the network is terminated in a reflectionless load, a_2 will be zero. Therefore from

$$a_2 = T_{21} a_1 + T_{22} b_1,$$

$$\frac{b_1}{a_1} = -\frac{T_{21}}{T_{22}}$$

but the ratio $\frac{\text{reflected wave}}{\text{incident wave}} = \text{reflection coefficient}$

or

$$\rho = \frac{T_{21}}{T_{22}}$$

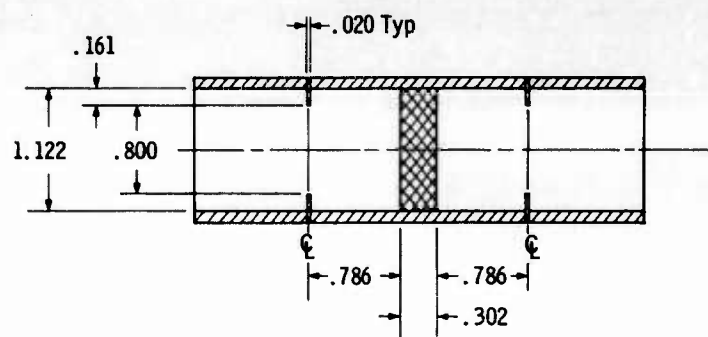
now

$$\text{VSWR} = \frac{1 + \rho}{1 - \rho}$$

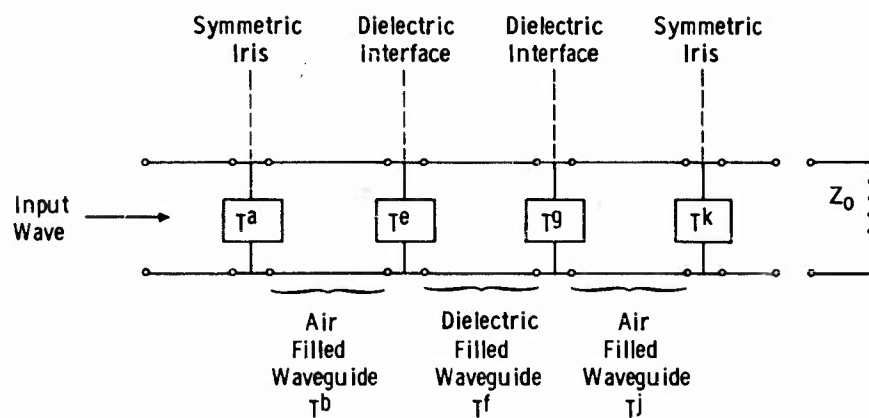
$$\text{VSWR} = \frac{1 + \frac{T_{21}}{T_{22}}}{1 - \frac{T_{21}}{T_{22}}}$$

The variables represented in the product $[T]$ are those of window dimensions, dielectric constant, and frequency.

A computer program was written for design optimization of the two windows discussed above. Windows of each type were then cold tested for comparison with the computer designed equivalent. Figure 33 shows the dimensions of the actual experimental window along with the computer model. This model needed only a seven matrix representation so the shunt admittances introduced by two of the four pairs of symmetric irises were set equal to zero. This is accomplished by letting "d" in $\cot \frac{\pi d}{2a}$ equal "a" making $\frac{B}{Y_0} = 0$.



(a) Actual BeO Block Window Dimension



(b) BeO Block Window Model

FIGURE 33
BERYLLIUM OXIDE WINDOW ACTUAL AND COMPUTER MODELS

thus

$$[c] = [i] \begin{bmatrix} 1 & 0 \\ 0 & 1 \end{bmatrix}$$

Similarly for the two unneeded waveguide section matrices $[d]$ and $[h]$. Dimension L in $e^{j\beta L}$ is allowed to go to zero,

thus

$$[d] = [h] \begin{bmatrix} 1 & 0 \\ 0 & 1 \end{bmatrix}.$$

The general computer program when used for this specific window is not affected if multiplied by these unit matrices. A comparison of results for a beryllia window is shown in Figure 34. The differences in the two curves are attributed to inaccuracies due to tolerance build up, and to variation in dielectric constant from the actual value.

An example of results from adapting the double thin disc program to the single disc case is shown in Figure 35. This adaptation is done by converting the unwanted matrices to unit matrices, as was done for the block window example. Quarterly Technical Note No. 4 reported these results as a comparison between identical windows with the exception that L_b (distance from transition to face of window) was .080 inch smaller in the measured window.⁴ A further analysis of the results showed that this difference would not have existed had the correct value of dielectric constant been used in the computation. This was another example of using an obsolete relative dielectric constant for a material which has been improved over a period of time. The manufacturer's published data indicate ϵ^1 equals 9.04 for AL300 and 9.37 for AL995. The average measured values for several dozen samples recently checked indicate ϵ^1 equals 9.45 for AL300 and 9.62 for AL995 at 8.0 Gc at room temperature. Other recent measurements* of the loss tangents and dielectric constants of beryllia and alumina ceramics indicate similar discrepancies in other manufacturers' published values. An abbreviated summary of these up-to-date measurements is included in Table V.

The trend toward increasing dielectric constant with passage of time can be attributed to improvements in the manufacturing processes of molding, and to the improved purity of today's ceramics. This cycle of improvement in ceramic quality and increase in dielectric constants has probably not yet reached the limit; therefore, it is recommended that in any design problem these constants should be determined for each new shipment of ceramic.

Another comparison of actually measured and calculated VSWR versus frequency characteristics is shown in Figure 36. The measured curve shows a sharp

* Quoted constants are from W. B. Westphal, Laboratory for Insulation Research, Massachusetts Institute of Technology, obtained October, 1963, by C. S. Pearsall of Varian, on a visit to MIT.

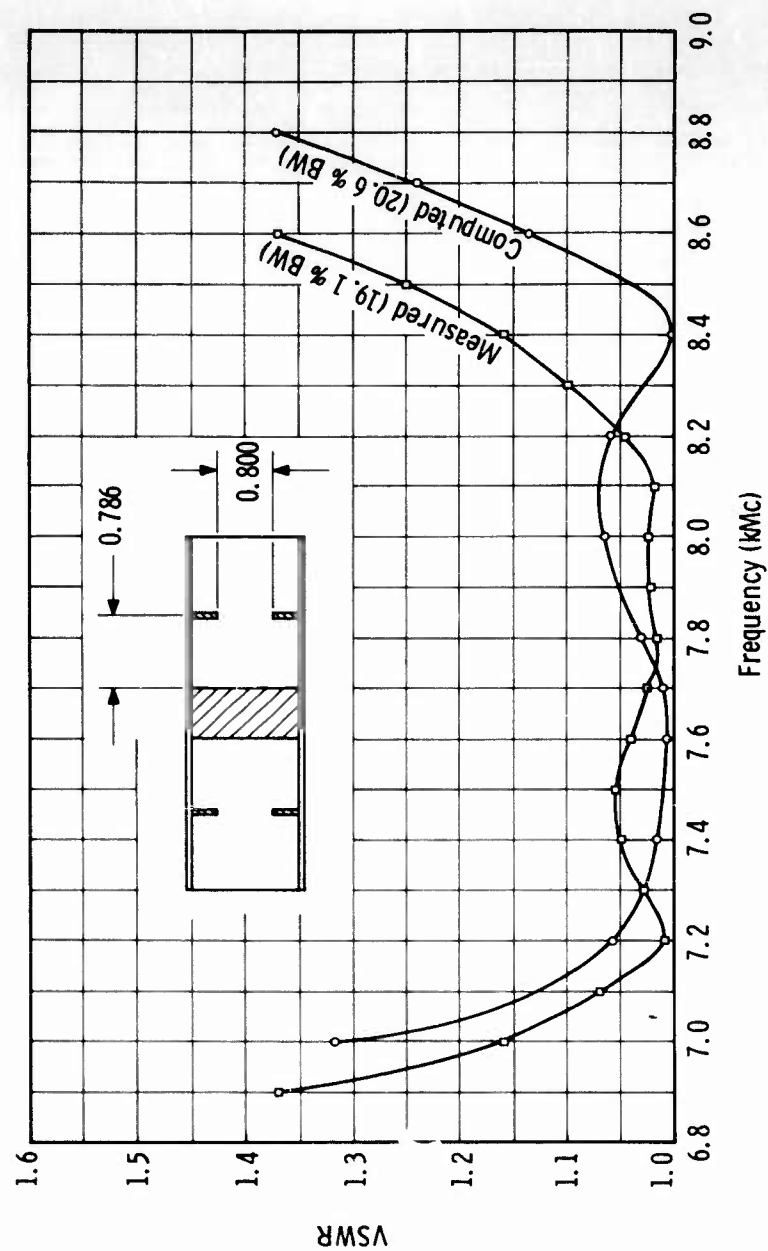


FIGURE 34
MEASURED AND COMPUTED RESULTS FROM BROADBAND
BERYLLIUM OXIDE WINDOW

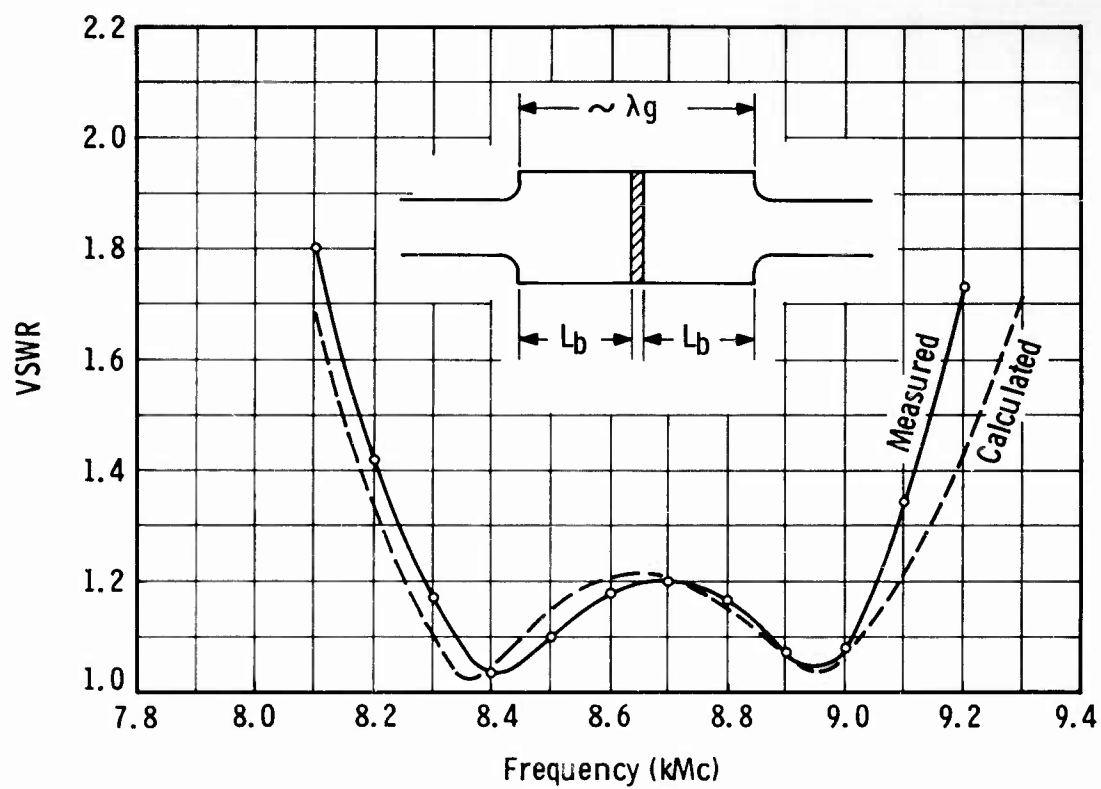


FIGURE 35
COMPUTED AND MEASURED VSWR CHARACTERISTICS OF A
THIN DISC λ_g LONG, CYLINDRICAL WINDOW

TABLE V

RECENT MEASUREMENTS OF MATERIAL CONSTANTS

MANUFACTURER	MANUFACTURE TYPE	COMPOUND	PURITY (percent)	DENSITY (gm/cm ³)	ϵ'	$\frac{\epsilon''}{\epsilon'}$
Wesgo	AL1009	Alumina	99.85	3.816	9.5	.000086
Wesgo	AL995	Alumina	99.5	3.758	9.37	.00021
Wesgo	AL300	Alumina	97.6	3.765	9.46	.00051
Wesgo	AL400	Alumina	95.0	3.687	9.19	.00072
Coors	AD995	Alumina	99.5	3.840	9.63	.00008
Coors	AD99	Alumina	99.0	3.795	--	.00020
American Lava	576	Alumina	--	3.277	8.19	.00120
American Lava	614	Alumina	96.0	3.725	9.30	.00080
American Lava	719	Alumina	94.0	3.586	8.99	.00094
Carborundum	1542	Alumina	--	3.726	9.21	.00048
Norton	--	Alumina	99.5	3.828	9.57	.00028
Diamonte	P3142-1	Alumina	95-97	3.706	9.18	.00065
Diamonte	B890-2	Alumina	90-95	3.583	8.74	.00115
Diamonte	P3662	Alumina	--	3.443	8.39	.00142
Minneapolis Honeywell	A203	Alumina	95.0	3.598	8.63	.00097
Minneapolis Honeywell	A127	Alumina	85.0	3.326	7.94	.00162
U. S. Stoneware	610	Alumina	--	3.832	9.43	.00008
U. S. Stoneware	212	Alumina	96.0	3.583	8.65	.00054
U. S. Stoneware	312	Alumina	96.+	3.508	8.47	.00080
U. S. Stoneware	216	Alumina	85.0	3.457	8.38	.000202
National Beryllia Corp.	Alox	Alumina	--	3.736	9.11	.00017
Brush Beryllia	B-7-6	Beryllia	--	2.791	6.48	.00050
Brush Beryllia	B-7-37	Beryllia	--	2.883	6.76	.00036
National Beryllia Corp.	--	Beryllia	--	2.822	6.59	.00044
High Temp. Materials Inc.	Pyrolytic	Boron Nitride	--	2.135	5.12	.00014
Carborundum	Hotpressed	Boron Nitride	--	2.06	4.777	.00033

All values at 25° C. Frequency range 3.140 to 4.870 Gc.

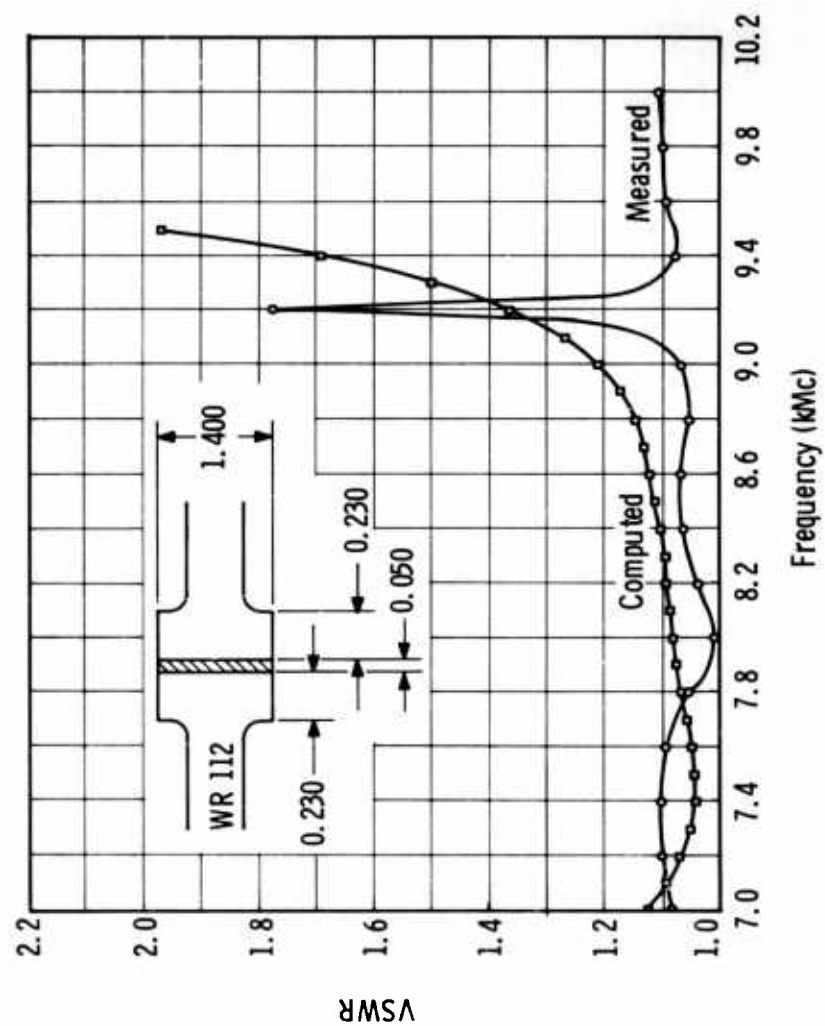


FIGURE 36
COMPUTED AND MEASURED VSWR CHARACTERISTICS OF A
SYMONS-TYPE SINGLE DISC AL300 WINDOW

resonant mode spike at 9.2 Gc and then falls again to a low value of VSWR at higher frequencies. The computed curve shows a flat response up to about 9.0 Gc, and then rises rapidly as frequency is increased. This thin disc window employed abrupt transitions only 0.230 inch from the face of the ceramic and had a total length of 0.510 inch between transition faces. The previous example using the same piece of ceramic had an overall length of 1.970 inches, or nearly 4 times as long. The calculations were both done assuming transmission only in the TE_{11}^0 mode.

These results would indicate very strongly that the thin disc, abrupt transition window propagates the TM_{11}^0 mode as well, particularly at the high end of the band. Cutoff frequency for the TM_{11}^0 mode is calculated to be 10270 Mc in air filled guide. Dielectric loading of the cylindrical cavity lowers this natural cutoff frequency. The close spacing of the abrupt transitions also materially aids in excitation and propagation of this mode through regions which are slightly below cutoff.

2-3. OBSERVATIONS ON MULTIPACTOR AND EVACUATED WINDOWTRON OPERATION

A. Conductive Coatings

Early in the program, plans were implemented to obtain and test windows coated with materials which would improve power handling capacity. These coatings would be designed to reduce secondary emission and to improve surface conductivity, thereby reducing multipactor or multipactor heating.

Several criteria were established for a good conductive coating material. They are:

1. Low vapor pressure
2. Stability in vacuum and hydrogen brazing atmospheres
3. Reproducible resistivity (1 megohm per square) under vacuum tube processing conditions
4. No cathode toxicity
5. Good bandability to dielectric substrate
6. Low loss in microwave frequency fields.

Work was begun with coatings of sesquioxide of vanadium, V_2O_3 , because it has all appearances of satisfying these criteria. Preliminary tests were made¹ with encouraging results. All was in readiness to high power test these coatings on a block window in a vacuum to determine effectiveness of multipactor suppression. During these preparations high power block window tests were performed as described previously, but no multipactor was either measured or seen in any of them. The persons involved with this test had considerable experience with multipactor effect measurements in Varian's evacuated S-band ring. In this test system high peak powers as well

as high average powers are available. Multipactor has been shown to be very definitely measureable by means of continuously monitoring heat dissipation in the test window. Some very interesting visual phenomena also occur with multipactor.

For example, a given window tested with pressurized gas at its faces would dissipate a given amount of power. At multipactor can occur only in a vacuum, a similar test on the same window with both faces in a vacuum showed that the heat lost is greater. Other tests gave results indicating multipactor is a discontinuous and irregular function of peak and average power levels. Dissipations measured on newly fabricated windows were always higher than those measured in the same window after they had been subjected to increasing amounts of power for an extended period of time. This suggests very strongly that an aging process for very high power windows subject to multipactor should be included in any tube processing.

Visible manifestations of multipactor are seen as variations in light patterns across the face of the window as power is varied over a given range. Colors of the lights vary from red to deep blue, depending on the ceramic and the power level. At intervals, as power is increased upwards over a wide range, the manifestations of multipactor will increase and decrease again only to appear in a different form or intensity at some higher power level.

This discussion has been entirely qualitative in nature in order briefly to describe phenomena not observed in any of the high average, but relatively low peak power measurements made during this program. It is thereby concluded that multipactor in high average power windows, up to 250 kilowatts cw, is a problem of no consequence. As power is increased beyond this level multipactor will certainly become apparent and from scaling of S-band results it is estimated that this threshold will occur between 0.3 and 1.0 megawatt.

Because no multipactor occurred, proposed work on reducing it by means of conductive coatings was suspended. However, the need for such coatings will undoubtedly be felt in future developments of even higher power systems which include waveguide windows.

B. Vacuum Testing

The use of a clear, transparent sapphire window as one half of the windowtron was an excellent choice for observation of the entire evacuated region between the windows. Every portion of the windows under test could be viewed by arranging the apparatus as shown in the sketch of Figure 37 and photograph of Figure 38. Both pressurized and vacuum sides could be continuously viewed through portholes on either end of the test section.

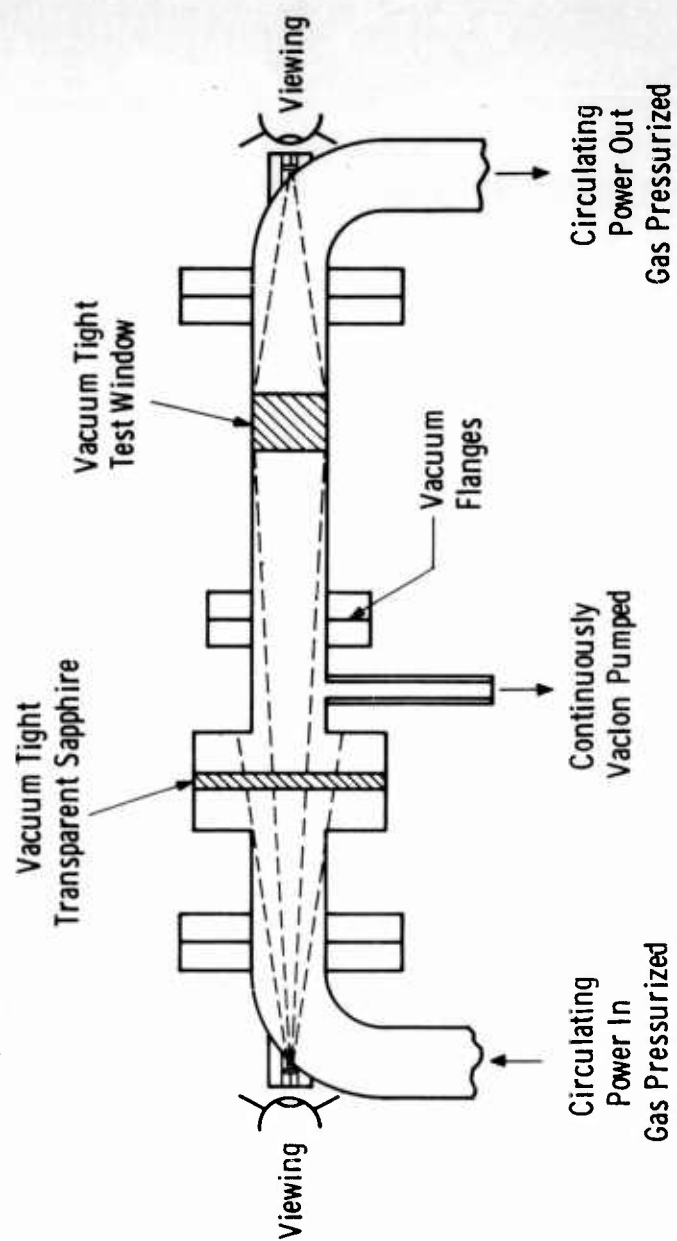


FIGURE 37
SKETCH SHOWING METHOD OF VISUALLY MONITORING
ALL TEST REGIONS

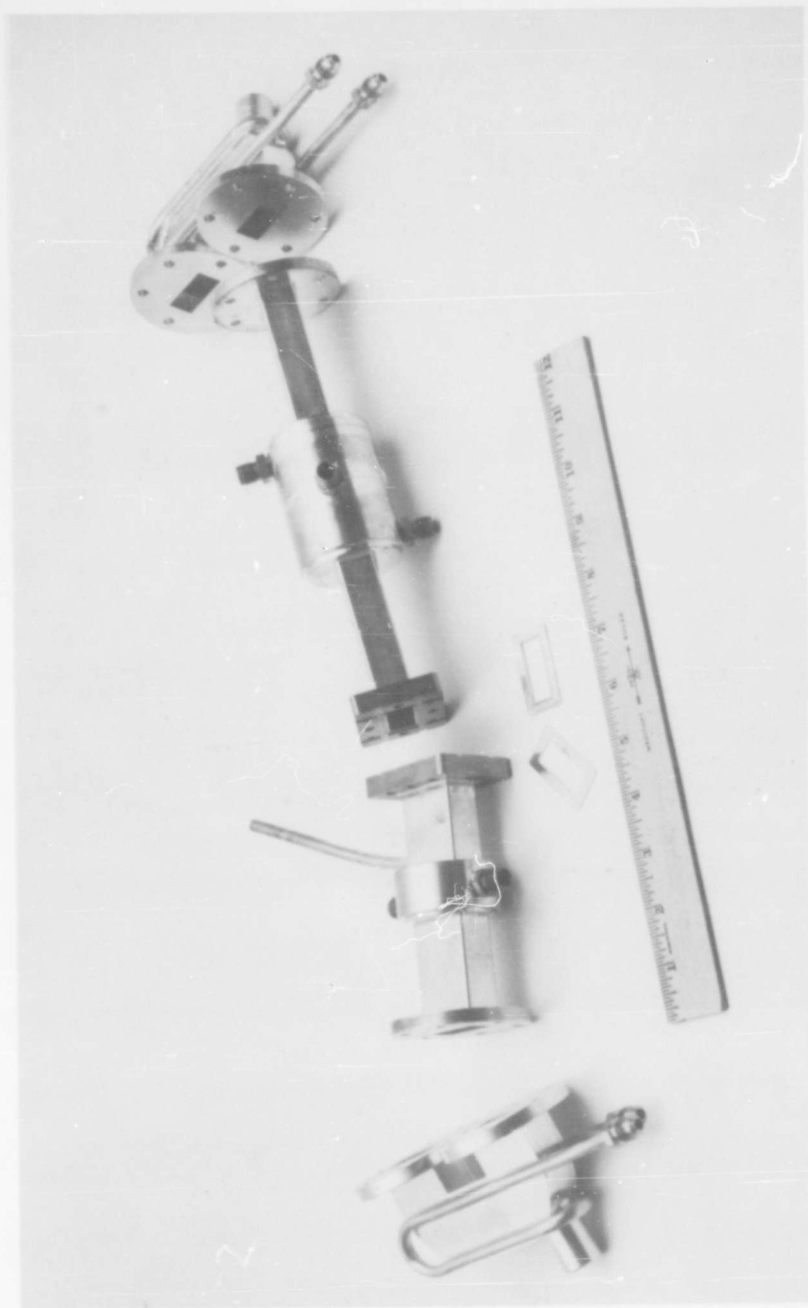


FIGURE 38
COMPONENTS OF WINDOWTRON ASSEMBLY

Two types of light-producing mechanisms were regularly seen in many of the high power tests. In the evacuated region any sharp, pinpoint edges protruding into the waveguide, no matter how small, would always become red hot and glow brighter with power increase. The slightest speck of dust or lint would also do the same but would eventually vanish. Waveguides which appeared very smooth and unmarred in any way to the naked eye were cluttered with pinpoint glows especially near the center of the waveguide. The size of points seemed to be magnified by r-f heating. Despite efforts to keep the waveguide absolutely clean and unscratched before evacuation, these glows could not be completely eliminated. As this phenomenon had no noticeable effect on test results and did not cause breakdown, attempts at micropolishing the waveguide were not made.

Another type of glow discharge was frequently seen in the pressurized portions of the waveguide. The power levels at which it occurred would vary anywhere from 30 kilowatts up, depending to some extent on the nitrogen pressure, but mainly on the temperature of the waveguide or window. Generally, when any portion of the waveguide became unusually hot, the gas would ionize in that immediate vicinity. The color of these discharges was always reddish blue and looked much like the familiar gas diode tube which is used in low voltage power supplies. It was this type of discharge that was seen in all of the quartz window tests. Apparently the very high temperatures shown to exist at the faces of those windows triggered the discharge. Poor flange connections became overheated on occasion and the discharge would occur at the flanges. Extinguishing potential was very low, requiring almost complete shutdown of the ring drive power to cease glowing.

Most of the evacuated window tests had a vacuum which ranged from 5×10^{-7} to 5×10^{-6} Torr at the highest power levels attained in any given test. The pressure in the sapphire-beryllia windowtron held fairly steady at 2×10^{-6} Torr when in the 250 kilowatt power range. These pressures were higher than the no-power pressures of about 1 or 2×10^{-7} Torr. In three of the windowtrons tested, pressure increased as high as 6×10^{-5} Torr. At this pressure level a faint hazy light seemed to fill the entire evacuated region and it became brighter as pressure increased until complete ionization occurred in the vicinity of 10^{-4} Torr. This effective short circuit automatically triggered the arc protection circuit in the ring driver, thereby shutting it off.

It was found that none of the windowtrons needed to be baked out prior to testing. Of course all due precautions were observed to keep each window clean after the final assembly brazing. In some cases small amounts of dust did manage to settle into the window, but they were soon removed by the action of high power and continuous ion pumping. The major source of trouble in vacuum testing came about as a result of dielectric-to-metal seal leaks and leaks due to improperly clamped flange connections. These would show up under high power tests when the waveguide temperatures caused uneven expansions in certain areas. In most cases the vacuum power experiments were no more difficult than the strictly pressurized tests. As trouble developed in a few cases, a small smear of high temperature varnish usually sealed the leak.

Small variations in pressure below 10^{-5} Torr caused no difficulty or adverse effects on the tests. When pressure increased another order of magnitude above this, satisfactory performance of the resonant ring was not possible.

C. Effects of Stray Magnetic Fields

Magnetic fields are used to focus electron beams in high power amplifier tubes. They are generally confined to the beam interaction regions, but in most cases some stray fields can be measured at more remote regions such as in the vicinity of the collector, output window, etc. For this reason an examination of the possible adverse effects of stray fields on evacuated waveguide and window operation was deemed advisable.

During the vacuum testing portions of the program, every effort was made to determine the effect of stray magnetic fields on operation of waveguide windows. Randomly polarized permanent magnets of various sizes were moved around the evacuated region. Some positions caused no effect. Others temporarily caused a faint glow of light to appear which then gradually disappeared. This was accompanied with a sudden burst of pressure as indicated on the VacIon current meter. The glow would disappear as pressure dropped. At any given power level the glow could not be introduced; however, by increasing the power level 5 or 10 kilowatts the glow would again appear and then disappear.

This procedure was repeated on the sapphire-beryllia windowtron up to a power level of 250 kilowatts, and each time the momentary glow would disappear. Other windows reacted in the same manner. The only conclusion reached as a result of these tests was that the magnets aided in the clean up of the windows and connecting waveguides. It was not possible to initiate sustained multipactor in any of the tests.

2-4. TEMPERATURE GRADIENTS IN WINDOWS

An effort was made early in the program to measure the approximate temperature gradients between the center of a block window and its outside edges. This was done for three different samples of ceramic (all in the same size of waveguide) as reproduced in Figure 39. The plots represent the temperature difference seen across a plane bisecting the narrow walls of the waveguide and running through the center of the ceramic.

The method employed to do this involved use of a crayon-like material called "Tempelstik." This product is made from a temperature-adjusted wax, and a thin layer of it may be applied to the surface of the ceramic without appreciably changing the electrical properties of the window. When power is transmitted through the window, the coating melts from the center outwards, but only to the points where the temperature is at or above the melting point of the particular crayon used.

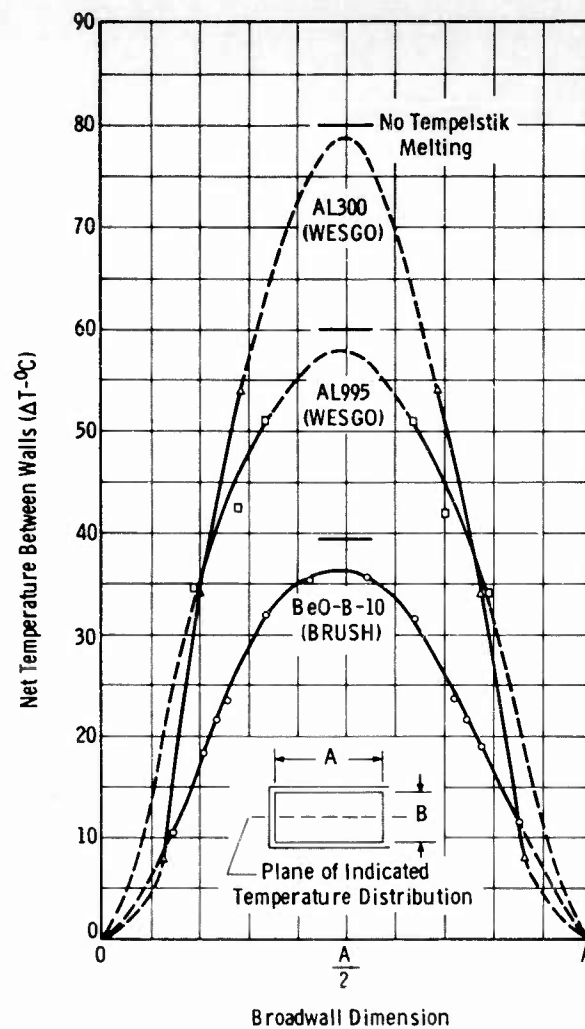


FIGURE 39
RELATIVE TEMPERATURE GRADIENTS OF VARIOUS
CERAMIC HALF-WAVELENGTH WINDOWS AT 100 KW

From measurement of the guide wall temperature with embedded thermocouples, the temperature rise across the window at a given power level can be estimated by measuring the width of the contour presented by the melted Tempelstik. Adjustment of flow rate and appropriate choice of melt temperature permit measuring contours for several guide wall temperatures and power levels until a combination is reached with no melting. This point represents an upper limit to the window temperature. Other variations in the application of Tempelstik include thin strips and dots, but results were essentially the same as that from a uniform thin layer. A photograph of typical results using a beryllia window is shown in Figure 40. The contours represent cooling and remelting of the Tempelstik as the power was increased. As would be expected, maximum heating occurs near the center, or the region of maximum power density.

A survey of the available literature on thermal stresses and their effect on ceramics was made but little or no work seems to have been done on problems resembling those presented by r-f heating of ceramics. The theories of shear and tensile stresses which have been advanced must all be modified by shape and restraint factors. Because of these, attempts at calculating theoretical temperature distributions and maximum stresses would probably be no more accurate than measurements made on this program. It has been determined that the alumina windows fail in the vicinity of 100 kilowatts, and inspection of these failures would indicate they were caused by very high tensile stresses. Often, particularly in the thin discs, crack separations of 0.010 or 0.020 inch can be seen. Kingery points out that maximum tensile stresses are generated in the center, while compressive stresses occur at the surface under heating.¹¹ Rigid restriction of ceramic in the waveguide compounds this compression. Restricted bodies such as metalized and brazed ceramic windows can have "stresses caused by differences in expansion between glaze... and the underlying ceramic or metal." With these factors considered it is not unreasonable to believe that temperature differences of 100°C or less could cause fracture in ceramic bodies, particularly if the thermal conductivity of the sample is low.

2-5. RING RESONATOR CONSIDERATIONS

As evidenced by the results of window testing mentioned in the preceding sections, the ring resonator is an invaluable piece of test equipment. Without it the kind of test program described herein could not be undertaken. For this reason some aspects of resonant ring performance will be considered here.

Before beginning work on this program, resonant ring window tests had been made for certain high power tube development projects at Varian Associates. The ring itself had been tested as a straight through piece of waveguide up to 300 kilowatts cw. Tuning of the ring to resonance, that is, where the ring is an integral number of guide wavelengths long, was done by adjustment of frequency. Actually, physical dimensions can be chosen so that a given ring will resonate very close to a design frequency for operation with a narrow band driver. This technique allows high power

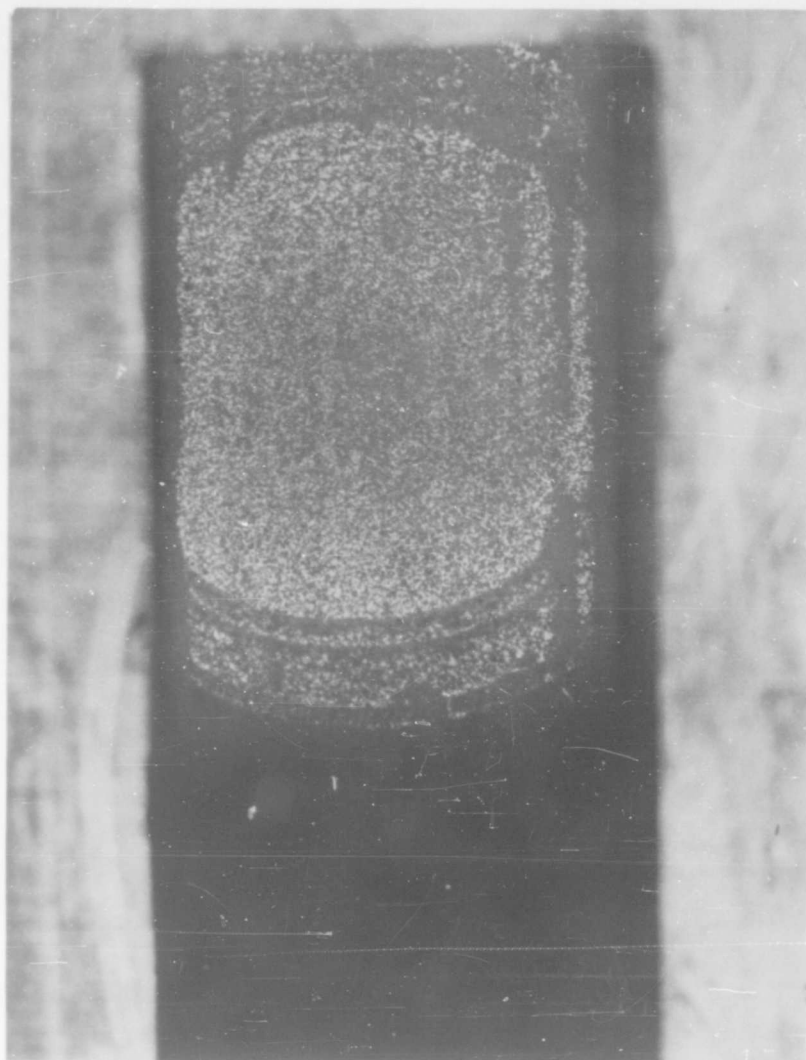


FIGURE 40
TEMPELSTIK MELTING CONTOURS OF
BERYLLIUM OXIDE BLOCK WINDOW

transmission through ordinary waveguide rather than through line stretchers of various types which have lower power breakdown thresholds. In this way the only limit to power transmission is the upper limit of the waveguide itself or perhaps the flange connections between various sections.

With drive power frequency to the ring set at resonance, further tuning is accomplished by a dual set of sliding short, hybrid phase shifters connected both at the input to the ring and to the output. Proper phasing of these two devices optimizes ring forward power and reduces ring back (reflected or reverse) power to a minimum.

Basically this was the routine followed for window tests during the first half of this program. However, it was reported that in some cases a great deal of arcing, pitting and overheating in the vicinity of these sliding shorts caused delays and even limitations to the maximum power attained. An analysis of the situation revealed that certain of the ring components had VSWR's of about 1.05, which in ordinary systems would be quite acceptable. At power levels in excess of 200 kilowatts, excessive reflected power was coupled back into the input waveguide. This was causing much of the difficulty.

Most of the back-power coupling was eliminated by placing small trimming irises as matching elements in each ring component. The match of each test window was also trimmed up so that the VSWR at the test frequency was 1.02 or less.

The results of succeeding tests showed that these simple precautions were well worth the effort. Not once since these modifications has it become necessary to repair the hybrid phase shifter sliding shorts. Other benefits have included much improved frequency stability and more insensitivity to thermal induced variations in the waveguide dimensions.

SECTION III

CONCLUSIONS

Two completely different window configurations have been shown by high power tests to be able to pass a minimum of 250 kilowatts, continuous wave X-band power, satisfying the study program requirements. A total of six window assemblies, three of each configuration, consistently passed the required tests.

Single crystal, zero degree cut, synthetic sapphire discs, using the Symons-type configuration, passed up to 275 kilowatts without failure. Bandwidth of these windows all exceed 25 per cent and power dissipation, 1.7 watts per kilowatt, was less than in any other metalized, vacuum sealed window. Considering the results, sapphire windows may hold only a slight edge over high purity beryllium oxide self-resonant block windows.

This latter configuration passed up to 263 kilowatts c-w power also without failure. Tests on beryllia blocks were performed under a wide range of conditions including pressurized and evacuated, narrow band and broad band waveguides with no measurable change in performance. Average dissipation in the beryllia blocks was 3.5 watts per kilowatt, or 0.35 per cent. The bandwidth of the beryllia window tested to 263 kilowatts was 20 per cent or somewhat less than the 25 per cent objective, but the significance of this result is that the broadbanding irises did not reduce the power capacity. High power tests on the above windows were limited only by available resonant ring drive power.

Another promising window not definitely proven to be capable of transmitting required power levels is the double disc fluid cooled window. Maximum power transmitted through a 33 per cent bandwidth version of this window was 180 kilowatts. Failure was concluded to be due to inadequate fluid flow. The coolant was FC-75, which has been considered too lossy for such applications; however, total window loss averaged only 8 watts per kilowatt transmitted in the several models tested. Further development of this window is indicated in order to improve the fluid flow rate for optimum cooling of the discs. This configuration has definite application in high average power systems because of its wide mode-free bandwidth, especially if made using some other materials such as sapphire. The double disc results reported herein were obtained from assemblies utilizing ordinary sintered aluminas, which have been shown to be inferior to sapphire or beryllia.

Double disc windows cooled by dry nitrogen gas fail prematurely because of inadequate cooling. It is concluded that air cooling of windows is too inefficient to be practical.

Exterior surface cooling of window assemblies of any variety was shown to be absolutely mandatory. Two double disc windows previously tested to approximately 160 kilowatts without failure promptly broke when subjected to 20 kilowatts without cooling of any kind. It should also be emphasized that waveguide sections must be very well cooled when operated at the power levels discussed in this report.

The upper limits of aluminum oxide windows in the block and single thin disc configurations have been established. Varieties of several aluminas, including the highest purity types available, when fabricated into block window all failed in test near the 100 kilowatt level. Use of aluminas for windows above this power level is not recommended. Single thin discs failed at power levels of less than 50 kilowatts when used in wideband configurations. Better results could be obtained using this material in thin disc, narrower band assemblies but the maximum is not expected to exceed 100 kilowatts. Power dissipation of alumina thin disc and block windows was identical: 3 watts per kilowatt transmitted.

It was established that the very low thermal conductivity of fused quartz limits its application to high average power windows. Very high quality optical grade quartz performed considerably better than commercial grades, but even so this material becomes visibly hot at power levels less than 200 kilowatts. Because of other problems associated with the sealing of fused quartz into vacuum-tight assemblies, this material should not be considered for very high average power windows.

Multipactor did not appear to be a problem at any power level up to and including the maximum testing level of 263 kilowatts in a vacuum. Attempts at artificially inducing sustained manifestations of this phenomenon by variations in randomly polarized magnetic fields were unsuccessful. Variations in vacuum pressure below 10^{-5} Torr did not produce a multipactor discharge. Above 10^{-4} Torr, operation of the ring resonator became impossible due to a discharge in the evacuated region of the windowtron. It can be concluded that multipactor, even in a vacuum poor by tube standards, is not a serious problem at or below the one-quarter megawatt, c-w power level.

The results of all tests indicate that the major reason for high average power window failure is poor thermal conductivity. This one property of a material seems to outweigh all other properties when considered for this application. The one exception to such a conclusion is sapphire, which exhibits an exceptionally high flexural strength. The strength factor would seem to overcome the deficiency in its thermal conductivity.

Table VI summarizes the maximum high power test results of the window study program. The fused quartz result is set off by itself because it was made with a compressive seal contrasted to metalized brazed seals of all the other windows.

TABLE VI			
SUMMARY OF MAXIMUM TEST POWER RESULTS OF VARIOUS WAVEGUIDE WINDOWS			
<u>Window Type</u>	<u>Maximum Power Transmitted (KW-CW)</u>	<u>Dissipation Rate (Watts/KW)</u>	<u>Type of Failure</u>
Sapphire Single Disc	275	1.7	None
Beryllia Block	263	3.5	None
Double Disc FC75 Cooled	180	8.0	Crack
Alumina Block	~100	3.0	Crack
Double Disc Gas Cooled	100	3.0	Melt and Crack
Alumina Single Disc	40	3.0	Crack
Fused Quartz Single Disc (Optical Grade)	180	1.4	Melt

SECTION IV

RECOMMENDATIONS

From this study program came some very positive results which established certain limitations on waveguide windows. The maximum power limitations on the two most successful windows, namely beryllia and sapphire, have not been determined. Further efforts to establish this limit should be made in light of the continued effort by RADC toward development of megawatt average power tubes. This will require upgrading of existing resonant ring testing facilities, but such a task is feasible considering the state of the art at the present time.

High thermal conductivity of window dielectrics is of prime importance and new materials exhibiting this property should be sought with all vigor. Materials such as boron nitride appear very promising in this respect despite its low flexural strength. If under high power test single crystal beryllium oxide is as much better than the polycrystalline beryllia as sapphire is better than polycrystalline aluminas, then the choice of window dielectric material would become rather obvious. However, single crystal beryllia is not now made in pieces large enough even for X-band application. Support of effort in this area is strongly indicated.

More effort should also be made towards improvement in fluids and fluid cooled windows. The handicap of using low thermal conductivity alumina ceramics can quite conceivably be overcome if proper and sufficient cooling methods can be devised for this material. An order of magnitude reduction of inert fluorocarbon fluid loss tangent would also be worth some effort.

Estimated power thresholds of multipactor in c-w windows is barely above the power levels attained in this program. For this reason conductive coating and multipactor limiting research should be pursued under conditions where actual testing can be performed.

REFERENCES

1. Quarterly Technical Note No. 1, "High Power R-F Window Study Program," Varian Associates for RADC under Contract No. AF 30(602)-2844.
2. Quarterly Technical Note No. 2, "High Power R-F Window Study Program," Varian Associates for RADC under Contract No. AF 30(602)-2844.
3. Quarterly Technical Note No. 3, "High Power R-F Window Study Program," Varian Associates for RADC under Contract No. AF 30(602)-2844.
4. Quarterly Technical Note No. 4, "High Power R-F Window Study Program," Varian Associates for RADC under Contract No. AF 30(602)-2844.
5. Final Technical Report, "High Average Power R-F Window Study," Sperry Gyroscope Company for RADC under Contract No. AF 30(602)-2428.
6. Second Quarterly Progress Report, "Investigation of Microwave Failure Mechanism and Their Elimination," Sperry Gyroscope Company for USAERDL under Contract DA 36-039 SC-87389.
7. S. Ramo and J. R. Whinnery, Fields and Waves in Modern Radio, (2nd ed.; Wiley, 1953), p. 463.
8. N. Marcuvitz, Waveguide Handbook, Radiation Laboratory Series, (New York: McGraw-Hill, 1951, Vol. 10), p. 221.
9. T. Moreno, Microwave Transmission Design Data, (New York: McGraw-Hill, 1948), p. 144.
10. J. E. Storer, L. S. Sheingold and S. Stein, "A Simplified Graphical Analysis of a Two Port Waveguide Junction," Proc. of IRE, Vol. 41, No. 8, Aug. 53, p. 1004.
11. W. D. Kingery, "Factors Affecting Thermal Stress Resistance of Ceramic Materials," Jour. of Amer. Ceramic Society, Vol. 38, No. 1, January, 1955, pp. 3-15.

DISTRIBUTION LIST

<u>Copy No.</u>	<u>No. of Copies</u>	<u>Address</u>	<u>Copy No.</u>	<u>No. of Copies</u>	<u>Address</u>
1	1	RADC RAT Griffiss AFB, NY	26	1	RADC RAUM Griffiss AFB, NY
2	1	*RADC RAALD Griffiss AFB, NY	27	1	RADC RAUO Griffiss AFB, NY
3	1	*RADC RAAPT Griffiss AFB, NY	28	1	RADC RAWC Griffiss AFB, NY
4	1	RADC RAL Griffiss AFB, NY	29	1	RADC P. 22 Griffiss AFB, NY
5	1	RADC RALC Griffiss AFB, NY	30	1	RADC RAWI Griffiss AFB, NY
6	1	RADC RALS Griffiss AFB, NY	31	1	RADC RAYA Griffiss AFB, NY
7	1	RADC RALT Griffiss AFB, NY	32	1	RADC RAI Griffiss AFB, NY
8	1	RADC RAO Griffiss AFB, NY	33	1	*RADC RAOL (Maj Shields) Griffiss AFB, NY
9	1	RADC RAD Griffiss AFB, NY	34-35	2	*RADC RAOL (S/L Tanner) Griffiss AFB, NY
10	1	RADC RAS Griffiss AFB, NY	36-38	3	Advisory Group on Electron Devices 346 Broadway, 8th Floor New York 13, NY
11	1	RADC RASG Griffiss AFB, NY	39	1	*AUL (3T) Maxwell AFB, Ala
12-15	4	RADC ROAMA (ROAEPP-1) Griffiss AFB, NY	40-59	20	*DDC (TISIA-2) Cameron Station Alexandria VA 22314
16	1	RADC GEELA (ROZMA)	60	1	Dr. Norman Moore Litton Industries 960 Industrial Road San Carlos, California
17	1	(ROZMC)	61	1	Mass Institute of Technology Research Laboratory of Electronics Cambridge 39, Mass. Attn: Document Library
18	1	(ROZME)	62	1	University of Minnesota Minneapolis, Minnesota Attn: Dr. W. C. Shepherd Dept of Elect Eng
19	1	(ROZMN)	63	1	Dr. M. Ettinberg, Polytechnic Institute of Brooklyn Microwave Research Inst Brooklyn 1, New York
20	1	* (ROZMCAT) Griffiss AFB, NY	64	1	Mr. John M. Osephchuk Raytheon Co Spencer Lab Burlington, Mass
21	1	RADC RASH Griffiss AFB, NY	65	1	Dr. W. M. Webster Director Electronic Research Lab RCA Labs Princeton, New Jersey
22	1	RADC RASS Griffiss AFB, NY			
23	1	RADC RAU Griffiss AFB, NY			
24	1	RADC RAUA Griffiss AFB, NY			
25	1	RADC RAUE Griffiss AFB, NY			

*Mandatory

DISTRIBUTION LIST (Cont.)

<u>Copy No.</u>	<u>No. of Copies</u>	<u>Address</u>	<u>Copy No.</u>	<u>No. of Copies</u>	<u>Address</u>
66	1	Stanford University Elect Research Laboratory Stanford, California Attn: Mr. D. C. Bacon Asst Director	82	1	NAFEC Library Bldg. 3 Atlantic City, N. J.
67	1	Dr. D. A. Watkins Stanford University Electronics Laboratory Stanford, California	83-87	5	*RADC (EMATE, Attn: D. Bussey) Griffiss AFB, NY
68	1	Secretariat Advisory Group on Electron Tubes 346 Broadway New York 13, New York	88	1	*RADC (RAAPT) Griffiss AFB, NY
69	1	Bell Telephone Labs Murry Hill Laboratory Murry Hill, New Jersey Attn: Dr. J. R. Pierce	89	1	*RADC (RAIS, Attn: Mr. Malloy) Griffiss AFB, NY
70	1	Mr. A. G. Pelfer Research Laboratories Div The Bendix Corporation Southfield Detroit, Michigan	90	1	US Army Electronics R and D Labs Liaison Officer RADC, Griffiss AFB, NY
71	1	Mr. John W. Sargent Product Manager Commercial Development Dept Chemical Division Minnesota Mining and Mfg. Co. 367 Grove Street St. Paul, Minnesota	91	1	*AUL (3T) Maxwell AFB, Ala
72	1	Professor R. M. Saunders University of California Dept of Engineering Berkeley 4, California	92	1	ASD (ASAPRD) Wright-Patterson AFB, Ohio
73-74	2	Commanding Officer US Army Signal R and D Lab Attn: Logistics Div (SIGRA/SL-PRT) L. N. Heynick Ft. Monmouth, New Jersey	93	1	Chief, Naval Research Lab Attn: Code 2027 Wash 25 DC
75	1	Field Emission Corp 611 Third Street McMinnville, Oregon Attn: Mr. F. M. Charbonnier	94	1	Air Force Field Representative Naval Research Lab Attn: Code 1010 Wash 25 DC
76	1	Dr. Robert T. Yang Chief Electron Tube Branch Diamond Ord Fuse Lab Washington 25, D. C.	95	1	Commanding Officer US Army Electronics R and D Labs Attn: SELRA/SL-ADT Ft Monmouth, NJ
77	1	Applied Radiation Co Walnut Creek, California Attn: Mr. Niel J. Norris	96	1	National Aeronautics and Space Admin Langley Research Center Langley Station Hampton Virginia Attn: Librarian
78	1	RTD (RTH) Bolling AFB Washington 25, D. C.	97	1	Central Intelligence Agency Attn: OCR Mail Room 2430 E Street NW Wash 25 DC
79	1	The Electronics Research Lab 427 Cory Hall The University of California Berkeley 4, California Attn: Mrs. Simmons	98	1	US Strike Command Attn: STRJ5-OR Mac Dill AFB Fla
80	1	Professor W. G. Worcester University of Colorado Dept. of Electrical Engineering Boulder, Colorado	99	1	AFSC (SCSE) Andrews AFB Wash 25 DC
81	1	Columbia University Columbia Radiation Lab 524 W 120th Street New York, N. Y.	100	1	Commanding General US Army Electronic Proving Ground Attn: Technical Documents Library Ft Huachuca Ariz
			101	1	AFSC (SCFRE) Andrews AFB Wash 25 DC
			102	1	Hq USAF (AFCOA) Wash 25 DC
			103	1	AFOSR (SRAS/Dr. G. R. Eber) Holloman AFB, NMex
			104	1	Office of Chief of Naval Operations (Op. 724) Navy Dept Wash 25 DC
			105	1	Commander US Naval Air Dev Cen (NADC Lib) Johnsville Pa

*Mandatory

DISTRIBUTION LIST (Cont.)

<u>Copy No.</u>	<u>No. of Copies</u>	<u>Address</u>	<u>Copy No.</u>	<u>No. of Copies</u>	<u>Address</u>
106	1	Commander Naval Missile Center Tech Library (Code NO 3022) Pt Mugu Calif	125	1	Dr. Louis R. Bloom Sylvania Elect Prod Inc Physics Lab 208-20 Willetts Point Blvd Bayside, Long Island NY
107	1	Bureau of Naval Weapons Main Navy Bldg. Wash 25 DC Attn: Technical Librarian, DL1-3	126-127	2	Technical Library Varian Associates 611 Hansen Way Palo Alto, California
108	1	Redstone Scientific Information Center US Army Missile Command Redstone Arsenal, Alabama	128	1	Dr. L. A. Roberts Watkins Johnson Co Palo Alto, California
109	1	Commandant Armed Forces Staff College (Library) Norfolk 11 VA	129	1	Mr. Gerald Klein, Mgr Microwave Tube Section Applied Research Dept Westinghouse Elect Corp Friendship Intl Airport Box 746 Baltimore, Md.
110	1	ADC (ADOAC-DL) Ent AFB Colo	130	1	Hughes Aircraft Co Culver City, Calif Attn: Everett M. Wallace
111	1	AFFTC (FTOOT) Edwards AFB Calif	131	1	Bendix Aviation Corp Red Band Division Eatontown, New Jersey Attn: John Johnstone
112	1	Commander US Naval Ordnance Lab (Tech Lib) White Oak, Silver Springs Md	132-133	2	Eitel Mc Cullough Inc 901 Industrial Way San Carlos, California Attn: Stella R. Vetter Research Library
113	1	Commanding General White Sands Missile Range New Mexico Attn: Technical Library	134	1	Mr. F. E. Ferrira Director of Research Coors Porcelain Co Golden, Colorado
114	1	Director US Army Engineer R and D Labs Technical Documents Center Ft Belvoir VA	135-136	2	Mr. M. Hoover RCA Lancaster, Pa
115	1	ESD (ESRL) L G Hanscom Fld Bedford Mass	137	1	Dr. D. Goodman Sylvania Microwave Tube Lab 500 Evelyn Avenue Mt. View, California
116	1	Commanding Officer and Director US Navy Electronics Lab (LIB) San Diego 52 Calif	138	1	Mr. A. E. Harrison University of Washington Dept of Elect Engineering Seattle 5, Washington
117	1	ESD (ESAT) L G Hanscom Fld Bedford Mass	139	1	Mr. Sheldon S. King Eng Librarian Westinghouse Elect Corp PO Box 284 Elmira, New York
118	1	Commandant US Army War College (Library) Carlisle Barracks Pa	140	1	Kane Engineering Labs 845 Commercial Street Palo Alto, California Attn: Mr. F. Kane
119	1	APGC (PGAPI) Eglin AFB Fla	141	1	Electrical Industries Co Murray Hill, New Jersey Attn: Mr. Peter A. Muto
120	1	AFSWC (SWOL) Kirtland AFB NMex	142	1	Mr. L. E. Gates, Jr. 20/1365 41-48-20 Hughes Aircraft Co Culver City, California
121	1	Dr. A. Prommer Litton Industries 960 Industrial Road San Carlos Calif			
122	1	Mr. Del Churchill Sperry Gyroscope Co Great Neck NY			
123	1	ARPA Attn: Col Lindsay Washington 25 DC			
124	1	RTD (RTOS) Bolling AFB Washington 25 DC			

DISTRIBUTION LIST (Cont.)

<u>Copy No.</u>	<u>No. of Copies</u>	<u>Address</u>	<u>Copy No.</u>	<u>No. of Copies</u>	<u>Address</u>
143	1	Mr. Theodore Poubanis Microwave Elect Prod Inc. Microwave Device Operations 600 Evelyn Avenue Mountain View, California	155	1	Dr. S. F. Katsel Microwave Electronics Corp 4061 Transport Street Palo Alto, California
144	1	Dr. R. G. E. Hutter Sylvania Microwave Tube Lab 500 Evelyn Ave Mt. View, California	156	1	Ohio State University Dept of Elect Engineering Columbus 10, Ohio Attn: Prof. E. M. Boone
145	1	Dr. William Watson Litton Industries 960 Industrial Road San Carlos, Calif	157	1	Mr. W. C. Brown Spencer Lab Raytheon Mfg Co Wayside Rd Burlington, Mass.
146	1	Technical Library Litton Industries 960 Industrial Road San Carlos, Calif	158	1	Mr. W. Teich Raytheon Mfg Co Spencer Lab Burlington, Mass.
147	1	Mr. Ted Moreno Varian Associates 611 Hansen Way Palo Alto, Calif	159	1	Mr. Hans Jenny RCA Elect Tube Div 415 South 5th Street Harrison, New Jersey
148	1	Mr. C. Dalman Cornell University Dept of Elect Eng Ithaca, New York	160	1	Mr. P. Bergman Sperry Corp Elect Tube Div Gainesville, Florida
149	1	Mr. Donald Priest Eitel-Mc Cullough Inc San Bruno, California	161	1	Dr. M. Chodorow Stanford University Microwave Lab Stanford, California
150	1	Mr. T. Marchese Federal Tele Labs Inc 500 Washington Ave Nutley, New Jersey	162	1	Dr. Bernard Arfin Varian Associates 611 Hansen Way Palo Alto, California
151	1	Mr. S. Webber General Elect Microwave Lab 601 California Ave Palo Alto, California	163	1	Dept of Electrical Eng University of Florida Gainesville, Florida
152	1	Mr. Lester Firestein Stanford Research Institute Palo Alto, California	164	1	Dr. E. D. Mc Arthur General Elect Co Electron Tube Div of Research Lab The Knolls Schenectady, New York
153	1	Dr. D. D. King Johns Hopkins University Radiation Laboratory Baltimore 2, Maryland	165	1	Mr. J. T. Milek Hughes Aircraft Co Electron Tube Laboratory Culver City, California
154	1	Mr. R. Butman M.I.T. Lincoln Laboratory PO Box 73 Lexington 73, Mass.	166	1	University of Illinois Electrical Eng Research Lab Urbana, Ill Attn: Technical Editor
			167-176	10	*ASTIA (TISIA-2) Arlington Hall Station Arlington 12 VA
			177-181	5	Retained by Varian Associates

*Mandatory

UNCLASSIFIED

UNCLASSIFIED